ELSEVIER

Coordination Chemistry Reviews
156 (1996) 91–138

COORDINATION CHEMISTRY REVIEWS

Annual survey of organometallic metal cluster chemistry for the year 1994

Michael G. Richmond

Center for Organometallic Research and Education, Department of Chemistry, University of North Texas, Denton, TX 76203, USA

Received 24 August 1995

Contents

Keywords: Cluster chemistry; Organometallic chemistry

1. Dissertations

The reaction between $Os(CO)_4L$ (where L is $CNBu^t$, PR_3) and $W(CO)_5(THF)$ gives the linear clusters $(OC)_4(L)OsOs(CO)_3(L)W(CO)_5$ and $(OC)_3(L)_2OsOs(CO)_4W(CO)_5$. The X-ray structure of the former cluster confirms the presence of the two dative metal–metal bonds in tandem (i.e. Os→Os→W). ^{13}C NMR data reveal that the solution structure is the same as that observed in the solid state. The

SSDI 0010-8545(95)01223-0

chemistry of the triangular clusters $Cp'Ir(CO)[Os(CO)_4]_2$ (where Cp' is Cp, Cp^*) is also included in this dissertation [1]. NOE studies on several osmium clusters have been conducted in order to determine the relative positions of chemically different hydride groups. T_1 spin lattice relaxation data have also been recorded, and the relationship between the T_1 values and the nature of the hydride correlated. The fluxional properties of $Os_3(CO)_{11}(L)$ (where L are Group 15 ligands in an equatorial site), $Os_3(CO)_{11}[Os(CO)_{5-x}(CNBu^t)_x]$ (where $x = 1, 2$), the kite-like cluster $Os_4(CO)_{15}$, and the three isomers of $Os_3(\mu\text{-}H)_2(CO)_9(CNBu^t)$ have been investigated by variable-temperature ^{13}C NMR spectroscopy [2]. Several polynuclear cluster compounds containing a Group 13 element have been synthesized and structurally characterized by X-ray crystallography. The unusual cluster $[Mn_{15}(CO)_{24}(THF)_{12}][Al(CH_3)_4(THF)]_2$, which was prepared from $Mn_2(CO)_{10}$ and $Al(CH_3)_3$, contains two planar Mn_7 arrays [3]. $[Ni_6(CO)_{12}]^{2-}$ reacts with Ph_3PAuCl to yield the nickel–gold cluster $[Au_6Ni_{12}(CO)_{24}]^{2-}$. The Au_6Ni_{12} polyhedron is based on five face-fused octahedra. The bonding in this cluster was explored by Fenske–Hall molecular orbital calculations, and the data were discussed relative to conventional electron-counting schemes. The same hexanickel starting cluster was examined for its reactivity towards $AsBu^tCl_2$. Several new nickel–arsinidene–carbonyl clusters have been isolated and characterized by X-ray crystallography. The variable-temperature ^1H NMR data for t-butylarsinidene exchange in $Ni_6(AsBu^t)_3(CO)_{10}$ are reported [4]. The oxo-bridged clusters $[(Ph_3P)_4Pt_3Rh(\mu_3\text{-}O)(COD)]^+$, $[(Ph_3P)_4Pt_2Au(\mu_3\text{-}O)L]^+$ (where L is phosphine), $[\{(Ph_3P)_4Pt_2(\mu_3\text{-}O)\}_2M]^+$ (where M is Cu, Ag) have been prepared. CO reacts with the gold–platinum cluster to afford the new cluster $[(Ph_3P)_8Pt_3Au(\mu\text{-}CO)_3]^+$ [5]. The silylformylation of 1-hexyne by several cobalt–rhodium clusters has been explored, with alkene and nitrile moieties remaining untouched [6].

The synthesis and characterization of the chromium cluster $[(\eta^5\text{-}C_5Me_4Et)Cr(\mu_3\text{-}H)]_4$ have appeared. Hydrogen reacts with this cluster to give $[(\eta^5\text{-}C_5Me_4Et)Cr(\mu_3\text{-}H)]_4(H)$ [7]. $LiBH_4$ reacts with $[Cp^*CoCl]_2$ to yield $[Cp^*Co)_3B_2H_4]$. This tricobalt cluster is transformed in moist air to $[(Cp^*Co)_3(H_2BH)(BOH)]$, while reaction in hot toluene with added $[Cp^*CoCl]_2$ affords $[(Cp^*Co)_3(H_2BH)(BCl)]$ [8]. Kinetic studies on the CO substitution in the carbide clusters $Ru_6C(CO)_{17}$ and $M_5C(CO)_{15}$ (where M is Fe, Ru) by $SbPh_3$, $AsPh_3$, and various phosphine/phosphite ligands are reported, and the concept of the "transition state isomer" introduced. The two pentanuclear clusters reveal the presence of a ligand adduct, which undergoes a subsequent loss of CO to give the observed product cluster $M_5C(CO)_{14}L$. The adoption of the square pyramid bridged butterfly square pyramid transformation is favored with ligands with cone angles less than 133°. Larger cone angle ligands display a different reaction sequence [9]. Reductive tetraplatinum condensation using *cis*-$Pt(PPh_3)_2Cl_2$ and $Pt(COD)Cl_2$/PR_3 (where R is Me, Et) with $Hg[Fe(CO)_3(NO)]_2$ leads to several new platinum–mercury carbonyl phosphine clusters. The geometry of these clusters is based on a tetraplatinum butterfly core [10]. The X-ray crystal structure of $Co_4(CO)_{9}(dppm)_2$ has been solved [11]. The chemistry of $[(MeCpMo)_2(\mu\text{-}S_2)(\mu\text{-}S)_2CoCp][I]_2$ has been explored in sulfur extraction reactions. The isoelectronic iron analog, $[(MeCpMo)_2(\mu\text{-}S_2)(\mu\text{-}S)_2FeCp][I]$, has also been prepared [12].

Triosmium and triruthenium clusters containing unusual ferrocenyl moieties have been prepared in pyrolytic reactions starting from either $M_3(CO)_{12}$ where M is Ru, Os) and the appropriate ligand or $M_3(CO)_{12-n}L_n$ (where $n = 1, 2, 3$). Reaction sequences involving Fe–M bonding, orthometalation, hetero-annular metalation, and P–C bond cleavages are presented for $M_3(CO)_{10}[Fc_2P^iPr_2]_2$, $Os_3(CO)_{11}(PFc_2Ph)$, $Os_3(CO)_{11}(PFc^iPr_2)$, and $Os_3(CO)_{11}(PFc_2Fc)$ are discussed. It is concluded that phosphine ligands on Ru_3 and Os_3 clusters are not totally inert [13]. Ruthenium and osmium clusters containing a benzynechromium tricarbonyl moiety are reported. Pyrolytic reactions leading to C–H and C–P bond activation in selected clusters are included [14].

The cluster $[Ni_3(\mu\text{-}CO)(\mu\text{-dmpm})_3]^{+}$ has been isolated as a product from the reaction of Ni(II)/dmpm in the presence of CO and $NaBH_3CN$ [15]. Comproportionation of $Ni(COD)_2$ and NiI in the presence of dppm affords the cluster $Ni_3(\mu_3\text{-}I)_2(\mu_2\text{-dppm})_3$ in high yield. The photochemical properties of this cluster have been examined, with photooxidation being observed at wavelengths shorter than 400 nm [16].

Warming a solution containing $Fe(CO)_3$(*cis*-cyclooctene)$_2$ and $(^iPr)_3SiPH_2$ from −40°C to room temperature affords the silylphosphinidene cluster $Fe_3(CO)_9(\mu\text{-}H)_2[\mu_3\text{-}PSi(^iPr)_3]$. Sequential deprotonation using $[Bu_4N][F]$ gives the dianionic cluster $[Fe_3(CO)_9(\mu_3\text{-}PSi(^iPr)_3)]^{2-}$ in THF solution. Use of CH_2Cl_2 as solvent leads to reaction at the silyl group and the cluster $[Fe_3(CO)_9(\mu\text{-}H)(\mu_3\text{-}PH)]^{-}$, through the cluster $[Fe_3(CO)_9(\mu\text{-}H)_2(\mu_3\text{-}P)]^{-}$. Desilylation also occurs with $CpFe(CO)_2Cl$ and R_3PAuCl (where R is Ph, Et) to give $Fe_3(CO)_9(\mu\text{-}H)_2[\mu_3\text{-}PFeCp(CO)_2]$ and $Fe_3(CO)_9(\mu\text{-}H)_2(\mu_3\text{-}PAuPR_3)$, respectively. The results of other functionalization studies, including several X-ray structures, are also presented [17]. Electrochemical data on the localized Fe–Fe bond cleavage in the bicapped *closo* cluster $Fe_3(CO)_9[\mu_3\text{-}PFeCp(CO)_2]_2$ are reported. The resulting cluster $[Fe_3(CO)_9[\mu_3\text{-}PFeCp(CO)_2]_2]^{2-}$, the product of two-electron reduction, has been characterized by IR spectroscopy and X-ray crystallography. It is shown that the intermediate radical $[Fe_3(CO)_9[\mu_3\text{-}PFeCp(CO)_2]_2]^{\cdot-}$ is unstable and disproportionates to starting material and dianion. The involvement of this cluster radical in electron-transfer-chain (ETC) catalysis is demonstrated. ETC reactivity studies using bidentate phosphine ligands are also presented [18]. The use of the cluster $Fe_3(CO)_9(\mu_3\text{-}PR)_2$ (where R is SiR_3, H) as bifunctional building blocks for the construction of cluster oligomers is described [19].

2. Homometallic clusters

2.1. Group 4 clusters

Reaction of organolithium and Grignard reagents with the oxo-bridged trimer $[Cp^*Ti(Cl)(\mu\text{-}O)]_3$ furnishes the new alkyl oxo trimers $[Cp^*Ti(R)(\mu\text{-}O)]_3$ and $[Cp^*Ti(\mu\text{-}O)]_3ClR_2$ in good yield. Thermal decomposition of $[Cp^*Ti(Et)(\mu\text{-}O)]_3$ at elevated temperature gives $[Cp^*Ti(\mu\text{-}O)]_3(\mu_3\text{-}CMe)$, which is the first paradigm of a d^0 (μ_3-alkylidyne) compound. The molecular structure of the new alkylidyne complex

has been established by X-ray crystallography [20]. Treatment of $[Cp^*Ti(Cl)(O)]_3$ with Me_3SnF affords the corresponding fluorinated derivative $[Cp^*Ti(F)(O)]_4$, which contains an eight-membered Ti_4O_4 ring [21].

2.2. Group 6 clusters

The trinuclear mixed-valence cluster $[(OC)_4MoS_2MoS_2Mo(CO)_4]^{2-}$ has been synthesized in high yield from the tetrathiomolybdate ion and the dithiocarbamate complex $[Mo(CO)_4(S_2CNEt_2)]^-$. This cluster was characterized by X-ray diffraction analysis, ^{95}Mo NMR spectroscopy, and cyclic voltammetry. The electrochemical data support the presence of two different metal redox centers [22]. Exhaustive thermolysis of $CpCr(CO)_3(FePh)$ leads to $Cp_4Cr_4Te_4$, $Cp_4Cr_4Te_3O$, $Cp_4Cr_4Te_2O_2$, and $Cp_4Cr_4TeO_3$. Three of these products have been structurally characterized [23]. Hydrogenolysis of $[(\eta^5\text{-}C_5Me_4Et)Cr^{II}(\mu\text{-}Me)]_2$ affords the paramagnetic tetramer $[(\eta^5\text{-}C_5Me_4Et)Cr^{II}(\mu_3\text{-}H)]_4$, the X-ray structure of which has been redetermined in order to clarify a compositional disorder associated with the original determination. The results of H/D exchange with this tetramer are discussed, and the data used in connection with the structure proof of the tetrahydride [24]. The pentanuclear compound $Cp^*_4Mo_5O_{11}$, formed from the reaction of $[Cp^*Mo(O)(\mu\text{-}O)]_2$, $[Cp^*Mo(CO)_2]_2$, and O_2, is shown to contain a $Cp^*Mo(O)_2$ moiety attached to a $[Cp^*Mo(\mu\text{-}O)]_3(\mu_3\text{-}O)_3Mo(O)_2$ unit by a bridging oxygen atom by X-ray analysis. The magnetic moment has been studied as a function of temperature, and when coupled with the NMR and EPR data, reveals the existence of a redox equilibrium involving a diamagnetic cluster and two paramagnetic forms of this cluster [25]. Treatment of the dimer $HW_2(CO)_4(THF)_2(NO)$ with PBu^t_3 gives the hydrogen-bridged cluster $[W_3(CO)_{13}(NO)(\mu\text{-}H)_2][HPBu^t_3]$ as one of three products. The cluster anion may also be isolated as its PPN salt from the reaction of $HW_2(CO)_9(NO)$ with $[HW(CO)_5][PPN]$. The addition of nucleophiles to $[W_3(CO)_{13}(NO)(\mu\text{-}H)_2]^-$ leads to the corresponding CO substitution product, which in the case of the PMe_3-substituted derivative has been structurally characterized (Fig. 1) [26].

2.3. Group 7 clusters

Alkaline titration of $[Re(H_2O)_3(CO)_3]^+$ gives the rhenium(I) hydroxo compounds $[Re_3(\mu_3\text{-}OH)(\mu\text{-}OH)_3(CO)_9]^-$ and $[Re_2(\mu\text{-}OH)_3(CO)_6]^-$. The molecular structures of these products were confirmed by X-ray crystallography [27]. The temperature-programmed decomposition of $[Re(CO)_3OH]_4/Al_2O_3$ in a hydrogen atmosphere has been explored for methanation activity. Additional studies reveal that adsorbed methanol on the activated Re_4/Al_2O_3 sample is the source of the methane [28]. Polythiaether macrocycles have been prepared by thietane cyclo-oligomerization using the trirhenium cluster $Re_3(CO)_{10}[\mu\text{-}S\overline{CH_2CH_2CH_2}](\mu\text{-}H)_3$. Ring opening addition by added thietane furnishes the new clusters $Re_3(CO)_{10}[\mu\text{-}\underline{S(CH_2)_3}\overline{S(CH_2)_3}\underline{S(CH_2)_3}\overline{SCH_2CH_2CH_2}](\mu\text{-}H)_3$, $Re_3(CO)_{10}[\mu\text{-}S(CH_2)_3\overline{SCH_2CH_2CH_2(SCH_2CH_2CH_2)_2}\overline{SCH_2CH_2CH_2}](\mu\text{-}H)_3$, and $Re_3(CO)_{10}[\mu\text{-}S(CH_2)_3\overline{SCH_2CH_2CH_2(SCH_2CH_2CH_2)_4SCH_2CH_2CH_2}](\mu\text{-}H)_3$, in yields dependent on the amount

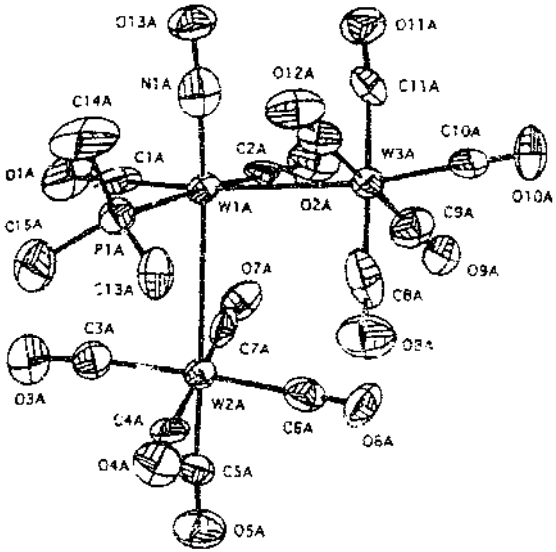

Fig. 1. Structure of the PMe_2-substituted derivative of $[W_3(CO)_{13}(NO)(\mu\text{-}H)_3]^-$. Reprinted with permission from Inorganic Chemistry. Copyright 1994 American Chemical Society.

of thietane employed. All three of these trirhenium clusters were fully characterized in solution by IR and NMR spectroscopy, in addition to X-ray crystallography in the case of the starting cluster and the first cyclo-oligomerization product (as the PMe_2Ph derivative). One of the many mechanistic schemes presented for thietane cyclooligomerization is shown below (Scheme 1) [29].

The hexanuclear cluster $[Re_6(CO)_{18}H_2]^{2-}$ has been isolated from the reaction between $Re_4(CO)_{12}H_4$ and $[Et_4N][BF_4]$. X-ray crystallography shows that the product is a non-carbide stabilized octahedral cluster, with face-bridging μ_3-hydride ligands [30]. Ferrocenium oxidation of $[Re_7C(CO)_{21}][PPN]_3$, followed by the addition of diazomethane, furnishes the carbene cluster $[Re_7C(CO)_{21}(\mu\text{-}CH_2)]^{3-}$, providing the first example of a methylene ligand in a higher nuclearity cluster. This particular cluster is readily decapped to give $[Re_6C(CO)_{18}(\mu\text{-}CH_2)]^{2-}$. The molecular structure of the heptarhenium cluster was established (Fig. 2), and the fluxional properties of both carbide clusters investigated by variable-temperature ^{13}C NMR spectroscopy [31].

2.4. Group 8 clusters

The surface-mediated synthesis of several neutral and anionic metal clusters has appeared. For example, $Os_3(CO)_{10}(H)(OH)$, $Os_4(CO)_{12}(H)_4$, $[Os_5C(CO)_{14}]^{2-}$,

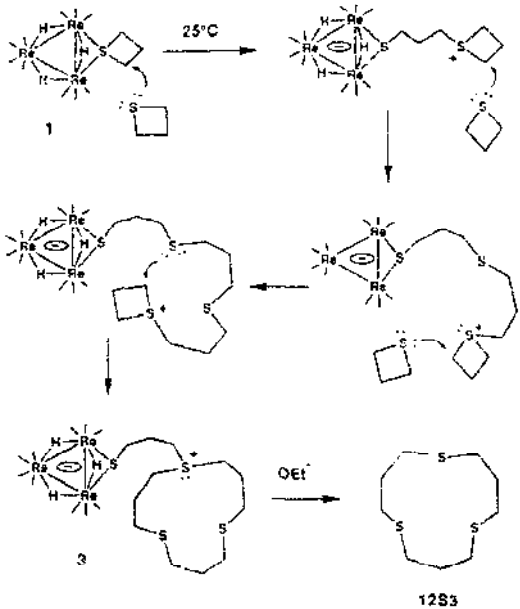

Scheme 1. Reprinted with permission from Journal of the American Chemical Society. Copyright 1994 American Chemical Society.

$[Os_{10}C(CO)_{24}]^{2-}$, $[Rh_5(CO)_{15}]^-$, and $[Pt_{15}(CO)_{30}]^{2-}$ have been prepared and the synthesis variables discussed [32]. The conversion of aqueous methyl formate to ethanol using ruthenium catalysts and PBu_3, which serves to activate the methyl formate, is reported. Selectivity aspects of this reaction are discussed and a catalytic mechanism involving the triruthenium cluster $[Ru_3(CO)_{11}(H)]^-$ is presented [33]. The data from a time-resolved IR study on the photo-induced fragmentation of $Ru_3(CO)_{12}$ have been published. Photodissociation of CO from $Ru_3(CO)_{12}$ furnishes the unsaturated cluster $Ru_3(CO)_{11}$, which is then shown to fragment further to $Ru(CO)_5$ and $Ru_2(CO)_9$ under the appropriate conditions, in addition to re-formation of the parent cluster. The observation of the transient species $Ru(CO)_4$(solvent), $Ru_2(CO)_8$, and $Ru_3(CO)_{12}(\mu$-CO) is also discussed [34]. $Ru_3(CO)_{12}$-catalyzed reductive carbonylation of *ortho*-nitrobiarenes and dinitrobiarenes gives the corresponding amines and five-membered heterocyclic indoles and imidazoles. Pertinent organoruthenium intermediates are presented on the basis of force-field calculations [35]. The reaction of $Os_3(CO)_{12}$ and $Ru_3(CO)_{12}$ with the silanol groups of silica gives the supported clusters $M_3(CO)_{10}(\mu$-H)(μ-OSi$\equiv$). These surface-supported clusters have been explored for their catalytic activity in alkane hydrogenolysis reactions, olefin isomerizations and hydrogenations, Fischer–Tropsch synthesis, and the water–gas

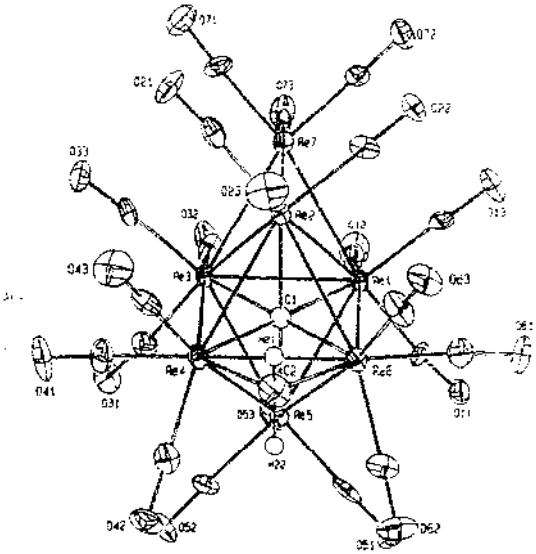

Fig. 2. Structure of the heptarhenium complex $[Re_7C(CO)_{21}(\mu\text{-}CH_2)]^-$. Reprinted with permission from Organometallics. Copyright 1994 American Chemical Society.

shift reaction [36]. 1-Hexene hydroformylation has been investigated by using $Ru_3(CO)_{12}$ and bpy on several inorganic supports. Of the several conclusions reached by this work, one was that the nature of the catalyst is best regarded as being heterogeneous [37]. Low-temperature X-ray structures of $Fe_3(CO)_{10}(\mu\text{-}CO)_2$ have revealed that the bridging carbonyls become more symmetric, coupled with the shortening of the carbonyl-bridged Fe–Fe bond, as the temperature is lowered. The cluster possesses nearly exact C_{2v} symmetry at 100 K, which was the lowest temperature employed in the data collection [38,39]. $Os_3(CO)_{12}$ and excess diphenylacetylene react under photolysis ($\lambda < 370$ nm) to afford $(\eta^4\text{-}C_4Ph_4CO)Os(CO)_3$. The X-ray structure of this $(\eta^4\text{-}2,3,4,5\text{-tetraphenylcyclopenta-2,4-dien-1-one})$osmium species was established and compared with the iron and ruthenium congeners [40]. Treatment of (*Z*)-1,1-dimesityl-2-neopentylidenesilirane with $Ru_3(CO)_{12}$ leads to the triruthenium hydride cluster $Ru_3(CO)_8[\mu_3\text{-}Mes_2Si(C{-}CHBu^t)C_2O](\mu\text{-}H)_2$ as the major product. X-ray crystallography confirms the presence of the capping 1-oxa-2-silacyclopentene moiety (Fig. 3). The insertion of CO into the silirane is discussed [41].

The results of ab initio molecular orbital calculations on $Cp_3Ru_3(\mu_3\text{-}H)_2(\mu\text{-}H)_3$, $[Cp_3Ru_3(\mu\text{-}H)_6]^+$, and $Cp_3Ru_3(\mu\text{-}H)_3$, along with the rearrangement of the alkyne ligand in $Cp_3Ru_3(\mu\text{-}H)_3(\mu_3\text{-}\eta^2\text{-}HCCR)$, have been published. The triruthenium framework in these clusters is stabilized predominantly by three-center two-electron

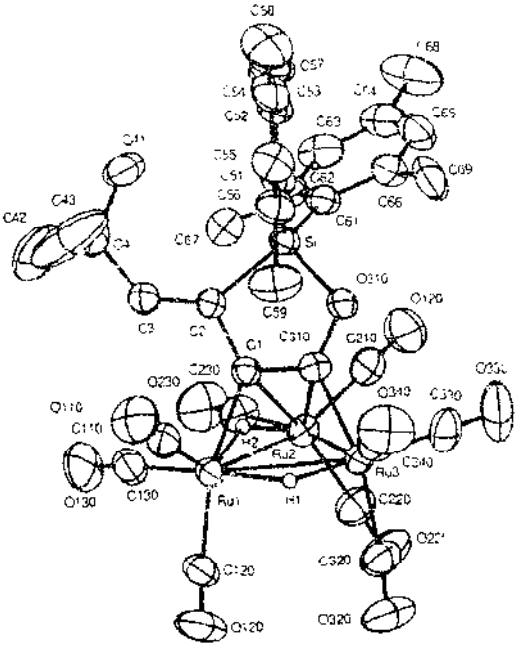

Fig. 3. Structure of 1-oxa-2-silacyclopentene substituted cluster. Reprinted with permission from Organometallics. Copyright 1994 American Chemical Society.

Ru–H–Ru bonds, and the perpendicular conformation in the alkyne clusters has been found to be more stable than the parallel conformation [42]. The mechanism of hydride exchange in the clusters $M_3(CO)_9(\mu\text{-}H)_3(\mu_3\text{-}CH)$ (where M is Ru, Os) has been investigated by using ab initio molecular orbital calculations. It is proposed that hydride exchange takes place in multiple steps by two energetically competitive pathways, the nature of which is fully discussed [43]. A report describing the selective carbon–carbon bond cleavage of cyclopentadiene by the unsaturated cluster $Cp^*_3Ru_3(\mu_3\text{-}H)_2(\mu\text{-}H)_3$ has appeared. The resulting triruthenium 2-methylruthenacyclopentadiene cluster, $Cp^*_3Ru_3(\mu_3\text{-}H)_3[\mu_3\text{-}\eta^4\text{-}C(Me)\text{=}CHCH\text{=}CH]$, arises from the scission of the $C(sp^2)$-$C(sp^3)$ bond of cyclopentadiene. The molecular structure of this polynuclear metallocycle was determined by X-ray crystallography (Fig. 4). The report represents the first example of selective activation of an unactivated C–C bond promoted by three metal centers [44].

The reaction of $Ru_3(CO)_{12}$ with oxadienes is reported to give tri- and hexa-nuclear ruthenium clusters containing a five-membered oxaruthenacycle moiety [45]. $Ru_3(CO)_{12}$ reacts with 4-methoxyphenol and 2-naphthol to give new tetra- and hexa-

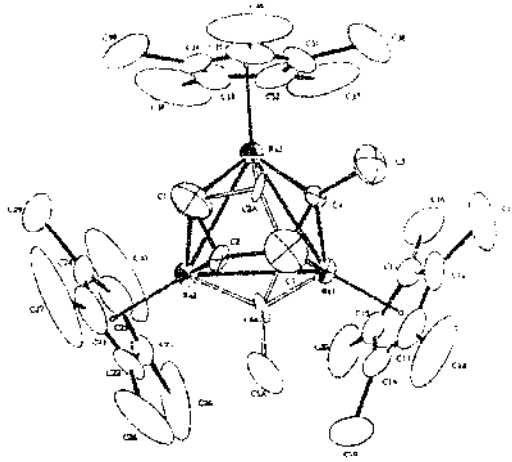

Fig. 4. Structure of $Cp^*Ru_4(\mu_3\text{-}H)_2\{\mu_3\text{-}\eta^2\text{-}C(Me)\text{=}CHCH_2\}(CH_2)$. Reprinted with permission from Journal of the American Chemical Society. Copyright 1994 American Chemical Society.

nuclear ruthenium clusters. All clusters have been characterized in solution by IR and NMR spectroscopy, and the X-ray structure of the mixed-valence cluster $Ru_4(\mu_3\text{-}OC_6H_3OMe\text{-}4)(\mu\text{-}Cl)(\mu\text{-}OC_6H_3OMe\text{-}4)(CO)_{10}$ is presented [46]. $Ru_3(CO)_{12}$ has been allowed to react with catechol and 3,5-di-*tert*-butyl-1,2-benzoquinone to yield the clusters $Ru_3(CO)_8(\mu_3\text{-}O_2C_6H_2R_2)_2$ (where R is H, Bu^t), which differ in the arrangement of the ruthenium atoms. CO substitution in these clusters by added MeCN, PPh_3, THF, and diphenylacetylene occurs readily using the oxidative-decarbonylation reagent Me_3NO. The redox properties of these clusters were studied by cyclic voltammetry [47]. The oxidative addition of catechol to $Ru_3(CO)_{12}$ yields either $[Ru_3(\eta^2\text{:}\eta^6\text{-}\mu_2\text{-}O_2C_6H_4)(CO)_4]_2$ or $[Ru_3(\eta^2\text{:}\eta^6\text{-}\mu_2\text{-}O_2C_6H_4)(CO)_8]_2$, depending upon the reaction conditions. These clusters fragment to the mononuclear complexes $Ru(\eta^2\text{-}O_2C_6H_4)(CO)_3L_2$ (where L is phosphine or arsine) and $Ru(O_2C_6H_4)(CO)_n(py)_{5-n}$ (where $n = 1,2$), or the $\eta^2\text{-}\pi$ complexes $Ru_3(\eta^2\text{:}\eta^4\text{-}\mu\text{-}O_2C_6H_4)(CO)_4L_2$ in the presence of added ligand. All new complexes have been characterized in solution by IR and NMR spectroscopy, and by X-ray crystallography in selected cases. The redox properties of these complexes have been examined by cyclic voltammetry [48]. *ortho*-Halophenols react with $Ru_3(CO)_{12}$ in the presence of Me_3NO to produce the triruthenium clusters $Ru_3(CO)_8(\mu\text{-}\eta^2\text{-}OC_6H_3X)_2$ (where X is F, Cl, Br). X-ray data on the chloro derivative reveal that the *o*-OC_6H_4Cl ligands bridge one edge of the cluster framework and serve as five-electron donor groups. The reversible CO addition reactivity, which occurs at the expense of the Ru–X bond, and the ligand substitution chemistry exhibited by these clusters are discussed.

Reaction of pyridinecarbinol with $Ru_3(CO)_{12}$ proceeds similarly, giving $Ru_3(CO)_8(\mu\text{-}\eta^2\text{-}OCH_2C_5H_3N)_2$, the X-ray structure of which is shown below (Fig. 5) [49].

Variable-temperature ^1H and ^{13}C NMR studies have been conducted on $Os_3(CO)_{10}(\mu\text{-}H)(\mu\text{-}CH_3)$. The proton and carbon NOE and T_1 spin-lattice relaxation data on the methyl and methylene tautomers of this cluster have allowed for the inter-proton distances to be calculated. Parallel NMR studies on $Os_3(CO)_9(\mu\text{-}H)_3(\mu_3\text{-}CH)$ are also reported [50]. A ^{13}C-2D EXSY study on $Os_3(CO)_{11}(\mu\text{-}H)(H)$ has revealed the existence of a low-energy process involving the intramolecular exchange between two enantiomeric structures of this cluster. The newly discovered exchange process occurs prior to the known axial/equatorial hydride exchange exhibited by this cluster [51].

The cyclic voltammetric behavior and IR spectroelectrochemical characterization of the radical anion of $Os_3(CO)_{10}(bpm)$ and $Os_3(CO)_{10}(bpm)Re(CO)_3Br$ are reported. Whereas an Os–Os bond is broken upon reduction in the former cluster, the Os–Re cluster is shown to remain intact upon electron accession [52]. Ethylene reacts with $Os_3(CO)_{10}(PPh_3)(\mu\text{-}H)_2$ to produce the ethylidene cluster $Os_3(CO)_8(PPh_3)(\mu\text{-}H)_2(\mu\text{-}CHCH_3)$ as opposed to the previously claimed ethylene complex $Os_3(CO)_9(PPh_3)(\mu\text{-}H)(H)(C_2H_4)$. ^1H NMR data have established the presence of the ethylidene moiety, and 1-D and 2-D ^{13}C NMR experiments have revealed the relative positions of the ancillary CO, ethylidene, hydride, and phosphine ligands about the cluster polyhedron [53]. The dimerization of trimethylsilylpropyne on a

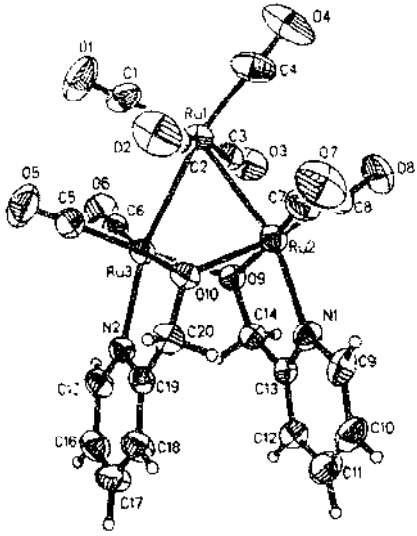

Fig. 5. Structure of $Ru_3(CO)_8(\mu\text{-}\eta^2\text{-}OCH_2C_5H_4N)_2$. Reprinted with permission from Inorganic Chemistry. Copyright 1994 American Chemical Society.

triosmium cluster has been reported. The details of the dimerization reaction are discussed, along with the synthesis and X-ray structure of $Os_3H[\mu_3$-$C(SiMe_2)C(Me)CC(SiMe_2)CH_2](CO)_8$ [54]. Several new silyl-substituted triosmium clusters have been prepared and crystallographically characterized. The new clusters are derived from 2-pyridyldimethylsilane [55]. Pentafluoronitrosobenzene reacts with $Os_3(\mu$-$H)H(CO)_{10}(EPh_3)$ (where E is P, As, Sb) to afford $Os_3(\mu$-$H)(CO)_{10}(EPh_3)(ONC_6F_4O)$, as a result of oxidation at the *para* position of the arene ring. The molecular structure of the phosphorus analog is presented [56]. Treatment of $(\mu$-$H)Os_3(CO)_{10}(\mu$-COMe) with dppl affords the corresponding substituted cluster $(\mu$-$H)Os_3(CO)_8(\mu$-COMe(dppf), which upon thermolysis leads to $(\mu$-$H)_2Os_3(CO)_7(\mu$-COMe)[μ-η^5-$(\eta^5$-$C_5H_3PPh_2)Fe(\eta^5$-$C_5H_4PPh_2)$, the X-ray structure of which accompanies this report [57]. The cluster $Ru_3(CO)_6(\mu_3$-$PPhCH_2PPh_2)(\mu_3$-CyNC)(CyNC)$_2$(Ph) has been obtained from the thermolysis of $Ru_3(CO)_{10}$(dppm) and CyNC. The molecular structure of this cluster was determined by X-ray crystallography [58]. Thermolysis of $Os_3(CO)_{11}$(CNR)(dppm) (where R is Pr, benzyl) in toluene leads to $Os_3(CO)$-(CNR)$(\mu$-$H)_2[Ph_2PCHP(Ph)C_6H_4]$, via the proposed intermediate $Os_3(CO)_8$(CNR)$(\mu$-$H)[Ph_2PCH_2P(Ph)C_6H_4]$, which has been isolated in the case of the propyl derivative. Thermolysis of the same starting cluster in the presence of added PPh_3 furnishes $Os_3(CO)_6(PPh_3)$ $[Ph_2PCH_2P(Ph)C_6H_4CNR]$, as a result of C–C bond coupling between the isonitrile and ortho-metalated phenyl group. The role played by the isonitrile ligand in this transformation is discussed, and the X-ray structures of several clusters are included [59]. The protonation chemistry of $Ru_3(CO)_{10}(\mu$-P P) (where P P is dppm, dppe, dppp, dppb) by CF_3CO_2H was examined for the site of [H]$^+$ addition. The case of protonation is discussed with respect to the nature of the bridging diphosphine ligand [60]. Four products have been isolated from the thermolysis of $Ru_3(CO)_{12}$ and 1,2-bis(phenylphosphino)benzene, of which $Ru_3(CO)_6[1,2$-$(\mu$-$PPh)_2C_6H_4]$, $Ru_3(CO)_7[1,2$-$(\mu$-$PPh)_2C_6H_4]_2$, and $Ru_4(CO)_{12}[1$-$(\mu_4$-P)-2-$(\mu$-$PPh_2)C_6H_4]$ have been structurally characterized by X-ray crystallography. The trirathenium cluster represents the first known tetraphosphido-stabilized 48-electron cluster. While this same cluster has been found to be stable in boiling mesitylene, CO substitution by PEt_3 occurs in THF to give two isomeric products [61]. Pyrolysis of the ferrocenylphosphine-substituted cluster $Ru_3(CO)_{12}(PFc_2Ph)$ gives $Ru_3(CO)_8(\mu$-$CO)(\mu$-$H)[\mu$-η^3-$(\eta^5$-$C_5H_3PFcPh)Fc(\eta^5$-$C_5H_5)]$ in 20% yield. The X-ray structure of this cluster is shown in Fig. 6. The reaction between $Ru_3(CO)_{12}$ and PFc_2Ph affords the clusters $Ru_3(CO)_{10}(\mu$-$CO)(\mu_3$-$PFc)(\mu$-η^3:η^5-$C_5H_4)$ and $Ru_4(CO)_{10}(\mu$-$CO)(\mu_4$-$PFc)(\mu_4$-$C_6H_4)$ in low yields. Also included in this report are the reactions of $PEtFc_2$ and PEt_2Fc with $Ru_3(CO)_{12}$ and the characterization of the resulting products [62].

The compounds $Os_3(pyS)_2(CO)_{10}$, $Os_3(pyS)_2(CO)_8$, $Os_3(pyS)_2(CO)_6$, $Os_3(CO)_8(H)(pyS)$, and $Os(pyS)_2(CO)_3$ have been isolated from the reaction between $Os_3(CO)_{10}(MeCN)_2$ and 2,2′-dipyridyl disulfide. The X-ray structures of the first four osmium compounds are presented, and the bonding modes exhibited by the pyridinyl sulfide ligand discussed [63]. The activation of (alkylthio)alkyne ligands by $Ru_3(CO)_{12}$ has been shown to give up to six types of products. The various ruthenium clusters formed have been characterized in solution by the usual methods

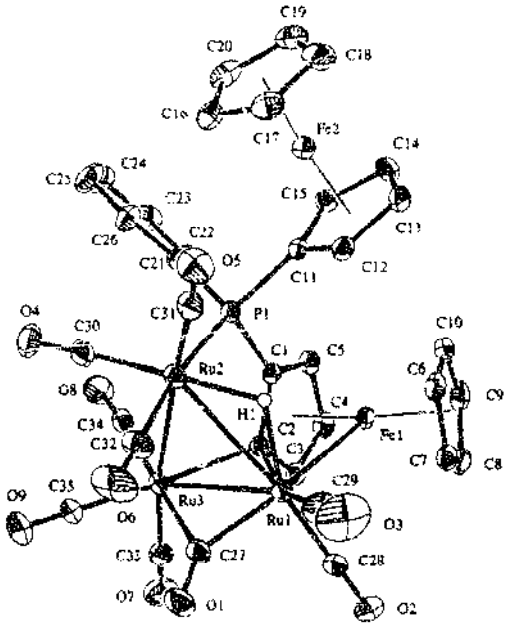

Fig. 6. Structure of $Ru_3(CO)_6(\mu\text{-}CO)(\mu\text{-}H)[\mu\text{-}\eta^2\text{-}\eta^5\text{-}C_5H_3(PPh_2)(\eta^5\text{-}C_5H_4)]$. Reprinted with permission from Organometallics. Copyright 1994 American Chemical Society.

and in the solid state by X-ray crystallography for selected examples. The results of extended Hückel molecular orbital calculations are presented and discussed relative to the polyhedral geometry adopted by the products [64]. The reaction of unsymmetrical thioalkynes with iron carbonyls leads to new tri-, tetra-, and penta-nuclear clusters [65]. The chalcogenide-bridged clusters $[Fe_3(CO)_{12}Te]^{2-}$ and $[Fe_3(CO)_{12}Se]^{2-}$ have been prepared. Both of these clusters transform into the corresponding Fe–Fe nido clusters $[Fe_3(CO)_9Te]^{2-}$ and $[Fe_3(CO)_9Se]^{2-}$, respectively, which have been structurally characterized by X-ray crystallography [66]. Treatment of $Os_3(CO)_{10}(MeCN)_2$ with phenylthiourea (HL^1) and *N,N'*-diphenylthiourea (HL^2) gives the sulfur-bridged clusters $Os_3(CO)_{10}(H)(\mu\text{-}L)$ (where L is L^1, L^2). Irradiation of these clusters with visible light leads to CO displacement by the nitrogen atom of the coordinated thiourea, giving the face-bridged clusters $Os_3(CO)_9(H)(\mu_3\text{-}L)$. The apparent activation energies and the quantum yields are reported, along with the X-ray structures of both *N,N'*-diphenylthiourea derivatives [67]. Treatment of the sulfido-capped cluster $Fe_3(CO)_9(\mu_3\text{-}S)_2$ with $M(\eta\text{-}dppf)_2$ (where M is Pd, Pt) gives the nido clusters $Fe_2(CO)_6(\mu_2\text{-}S)_2M(\eta\text{-}dppf)$, along with the substitution products $Fe_3(CO)_7(\mu_3\text{-}S)_2(\mu\text{-}dppf)$ and $[Fe_3(CO)_8(\mu_3\text{-}S)_2]_2(\mu\text{-}dppf)$

[68]. The sulfido-bridged clusters $Cp^*_2Fe_3(CO)_3(\mu_3\text{-}S)_2$ and $Cp^*_2Fe_2Ru(CO)_3(\mu_3\text{-}S)_2$ have been prepared from $Cp^*_2Fe_2S_4$ and various iron carbonyls [$Fe(CO)_5$, $Fe_2(CO)_9$, and $Fe_3(CO)_{12}$], and $Ru_3(CO)_{12}$, respectively. Both product clusters possess a *closo* polyhedral structure, as established by X-ray crystallography in the case of the triiron cluster [69]. Treatment of the tetramethylfulvene-bridged dinuclear complex $(\eta^1{:}\eta^5\text{-}CH_2C_5Me_4)Fe_2(CO)_6$ with CS_2 affords the trinuclear cluster $[(\eta^5\text{-}C_5Me_4)CH_2CS_2]Fe_3(CO)_8$ and $[\eta^5\text{-}C_5Me_4)CH_2CS_2]Fe(CO)_2$ as a result of C–C bond formation. X-ray crystallography of the triiron cluster shows that the dithiocarboxylato ligand $S_2CCH_2C_5Me_4$ bridges all three iron centers [70]. The kinetics of the interconversion of the parallel and perpendicular alkyne isomers in $Cp_2Fe_2(CO)_5(CF_3C{\equiv}CCF_3)$ have been explored. The effect of ancillary phosphine and phosphite ligands on the alkyne bonding has also been studied. Cyclic voltammetry data indicate that one-electron reduction leads to ligand loss (CO or P-ligand), followed by alkyne reorientation about the cluster framework, consistent with an EC process [71]. Alkylation of $[Fe_3(CO)_9(SO_2)(H)]^-$ by methyl triflate yields $Fe_3(CO)_9(SO_2CH_3)(H)$, as a result of oxygen alkylation. This product has been fully characterized in solution by IR and ^{13}C NMR spectroscopy, in addition to X-ray crystallography (Fig. 7). The X-ray structure reveals that the methyl group is bound to the *exo* oxygen atom of the coordinated SO_2 ligand. The nature of the SO_2–CH_3 interactions with the triiron framework has been investigated by extended Hückel molecular orbital calculations [72].

The solid-state reactivity of $Os_3(CO)_{10}(\mu\text{-}H)_2$ toward CO, NH_3, and H_2S has been explored and found to give the corresponding electron-precise clusters

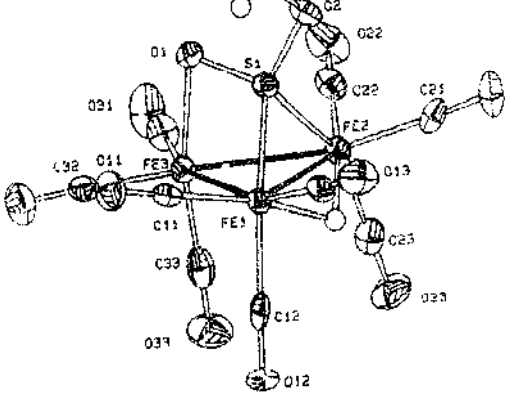

Fig. 7. Structure of $Fe_3(CO)_9(SO_2CH_3)(H)$. Reprinted with permission from Inorganic Chemistry. Copyright 1994 American Chemical Society.

$Os_3(CO)_{10}(L)(\mu\text{-}H)_2$. In the case where L is CO, the addition of CO was confirmed by ^1H magic angle spinning NMR spectroscopy. Two isomers for the NH_3-substituted product, which differ only in their orientation of the NH_3 and the terminal hydride ligands relative to the Os_3 plane, have been observed. The intermediate cluster $Os_3(CO)_{10}(H_2S)(H)_2$ transforms rapidly into the known cluster $Os_3(CO)_9(H)_2(\mu_3\text{-}S)$ [73]. The synthesis and X-ray diffraction structures of $Os_3(\mu\text{-}H)_2(CO)_9(\mu_3\text{-}CNC_5H_4CH{=}CH_2)$ and $Os_3(\mu\text{-}H)(CO)_9[\mu\text{-}C(H){=}NC_5H_4\text{-}\eta^2\text{-}CH{=}CH_2]$ have been published [74]. The linear clusters $Os_3Br(CO)_{10}(CNR)(\eta^3\text{-}C_3H_5)$ are prepared from the reaction of $Os_3(CO)_{10}(CNR)(MeCN)$ with allyl bromide. The X-ray structure of the propyl isonitrile derivative is included in this report [75]. The disorder of the carbonyl, CNPr, and MeCN groups in $Os_3(CO)_{10}(CNPr)(MeCN)$ has been investigated by X-ray crystallography [76]. Intramolecular [4 + 2] Diels–Alder cycloaddition products have been isolated from the reaction between $Os_3(CO)_{10}(H)_2$ and 2-(trimethylsilyl)-1-phosphabenzene and -1-arsabenzene. Besides the observed cycloaddition products $Os_3(CO)_9H[(Me_3Si)_2C_{10}H_5E_2]$ (where E is P, As), the clusters $Os_3(CO)_9H_2(Me_3SiC_5H_4E)$ have also been isolated. The X-ray structures of the latter phosphine derivative and the former arsine complex are presented, along with a working mechanism for the formation of these clusters [77]. A report on the synthesis and X-ray structure of (1,2,4,5-tetramethylenebenzene)$Fe_3(CO)_9$ has appeared. A brief discussion of the bonding of this disjoint, non-Kekulé biradical to the $Fe_3(CO)_9$ moiety is presented [78]. The new ruthenium clusters $Ru_3(\mu\text{-}H)(\mu\text{-}NC_5H_4)(CO)_9(PPh_3)$, $Ru_3(\mu\text{-}Cl)_2(NC_5H_5)(CO)_8(PPh_3)$, $Ru_3(\mu\text{-}Cl)_2(NC_5H_5)_2(CO)_8$ were obtained from the reaction between $Ru_3(\mu\text{-}AuPPh_3)(\mu\text{-}Cl)(CO)_{10}$ and pyridine. The latter two clusters have been structurally characterized by X-ray crystallography [79].

The trinuclear clusters $Ru_3(CO)_4(\mu\text{-}CO)(\mu_3\text{-}CO)(\mu_3\text{-}C_2R_2)Cp_2$ and $Ru_2Fe(CO)_5(\mu\text{-}CO)(\mu_3\text{-}CO)(\mu_3\text{-}C_2R_2)Cp_2$ (where R is Ph, CF_3) are synthesized in good yield from the reaction of the unsaturated ruthenium dimers $Ru_2(\mu\text{-}CO)(\mu\text{-}C_2R_2)Cp_2$ (Ru–Ru double bond) with $Ru(CO)_4$(ethylene) and $Fe_2(CO)_9$, respectively. These clusters exist as two geometric forms that are dependent on the π-coordination mode adopted by the alkyne ligand. The fluxional behavior of these clusters and selected X-ray structures are presented. The diphenylacetylene dimer $Ru_2(\mu\text{-}CO)(\mu\text{-}C_2Ph_2)Cp_2$ reacts with $Co_2(CO)_8$ to yield the 60-electron *closo* cluster $Ru_2Co_2(CO)_4(\mu_3\text{-}CO)_2(\mu_4\text{-}C_2Ph_2)Cp_2$, which has been shown by X-ray crystallography to contain a $Co_2Ru_2C_2$ octahedral core, with face-bridging μ_3-CO groups [80]. The reactivity of the triosmium cluster $Os_3(CO)_9(\mu\text{-}H)(\mu_3\text{-}\eta^2\text{-}C{=}NCH_2CH_2CH_2)$ with H_2, H_2S, and EtSH is described. The trihydride cluster $Os_3(CO)_8H(\mu\text{-}H)_2(\mu_3\text{-}\eta^2\text{-}C{=}NCH_2CH_2CH_2)$ is formed as the major product with H_2, and shows no sign of fluxional hydride behavior on the NMR time scale; however, the corresponding PPh_3-substituted cluster $Os_3(CO)_8(PPh_3)H(\mu\text{-}H)_2(\mu\text{-}\eta^2\text{-}C{=}NCH_2CH_2CH_2)$ exhibits dynamic hydride behavior that has been explored by variable-temperature ^1H and ^{31}P NMR spectroscopy. The cluster $Os_3(CO)_9H_2(\mu\text{-}H)(\mu_3\text{-}S)(\mu\text{-}\eta^2\text{-}C{=}NCH_2CH_2CH_2)$, which derives from H_2S, contains two cleaved Os–Os bonds [81]. Deprotonation of $(\mu\text{-}H)Fe_3(CO)_9(\mu\text{-}CO)(\mu_3\text{-}HBH)$ yields the spectroscopically characterized dianion $[Fe_3(CO)_9(\mu_3\text{-}HBCO)]^{2-}$, which

upon protonation decomposes. Reaction of the dianion with $FeCl_3$ leads to $[Fe_3(CO)_9(\mu\text{-}CO)(\mu_3\text{-}HBCl)]^-$, the structure of which has been determined by X-ray crystallography. A structural and reactivity comparison of these clusters with osmium derivatives and other isoelectronic clusters accompanies this report [82]. The reactivity of $[Ru_3(CO)_{10}(\mu\text{-}NO)][PPN]$ with tertiary silanes and stannes has been described [83]. The synthesis of the *cluster* "methylcyclopropenyl" cluster $Ru_3Cp^*_3[C_3H_2(CH_3)](\mu_3\text{-}CO)$ from the reaction between $[Cp^*RuCl]_4$ and *trans*-3-methyl-2-butenal is presented. The molecular structure of the resulting cluster was ascertained by X-ray crystallography [84]. The preparation and characterization of a variety of arene-substituted clusters have been described [85]. The synthesis and spectroscopic characterization of the [2.2]paracyclophane-substituted clusters $Ru_3(CO)_9(\mu_3\text{-}\eta^2{:}\eta^2{:}\eta^2\text{-}C_{16}H_{16})$, $Ru_6C(CO)_{11}(\mu_3\text{-}\eta^2{:}\eta^2{:}\eta^2\text{-}C_{16}H_{16})(\eta^6\text{-}C_{16}H_{16})$, and $Ru_6C(CO)_{13}(\mu_3\text{-}\eta^2{:}\eta^2{:}\eta^2\text{-}C_{16}H_{16})(\mu_2\text{-}\eta^2{:}\eta^2\text{-}C_6H_8)$ are reported. The X-ray structures of the latter two clusters are included, along with a comparison of these clusters to the known cluster $Ru_6C(CO)_{14}(\mu_3\text{-}\eta^2{:}\eta^2{:}\eta^2\text{-}C_{16}H_{16})$ [86]. Treatment of $Os_3(CO)_{10}(MeCN)_2$ with 1-hydroxybenzotriazole gives the hydride cluster $Os_3(CO)_{10}(\mu\text{-}H)[\mu_2\text{-}(2,3\text{-}\eta^2)\text{-}NNN(O)C_6H_4]$. Similar reactions were conducted with the isonitrile clusters $Os_3(CO)_{10}(MeCN)(CNR)$ (where R is Pr^n, benzyl), producing the bridging aminocarbyne clusters $Os_3(CO)_{10}[\mu_2\text{-}(2,3\text{-}\eta^2)\text{-}NNN(O)C_6H_4](\mu_2\text{-}\eta^1\text{-}C{=}NHR)$. Restricted rotation about the C=N double bond in the bridging amino carbyne ligand gives rise to regioisomers that have been characterized in solution by NMR spectroscopy. The X-ray structure of one of the three crystallographically characterized clusters is shown in Fig. 8 [87].

Carbon–phosphorus bond activation in both of the PPh_3 ligands in $Ru_3(\mu\text{-}H)(\mu_3\text{-}ampy)(PPh_3)_2(CO)_7$ occurs in boiling toluene under H_2 to afford the η^1-phenyl-bridged cluster $Ru_3(\mu\text{-}Ph)(\mu_3\text{-}ampy)(\mu\text{-}PPh_2)_2(CO)_6$. The results of X-ray data and extended Hückel calculations on this cluster are presented. Several other phosphine ligands were also examined, and were found to react in an analogous fashion. The related cluster $Ru_3(\mu\text{-}H)(\mu_3\text{-}mbim)(CO)_9$ reacts with PPh_3 in the absence of H_2 to give $Ru_3(\mu\text{-}Ph)(\mu_3\text{-}mbim)(\mu\text{-}PPh_2)_2(CO)_6$ [88]. Treatment of the 48-electron cluster $Ru_3(\mu\text{-}H)(\mu_3\text{-}\eta^2\text{-}ampy)(CO)_9$ with H_2 at elevated temperature produces the 92-electron hexaruthenium hexahydrido cluster $Ru_6(\mu\text{-}H)_6(\mu_3\text{-}\eta^2\text{-}ampy)_2(CO)_{14}$, the solid-state structure of which, as the P(*p*-tolyl)$_3$ derivative, has been determined by X-ray crystallography. The homogeneous hydrogenation of diphenylacetylene to *cis*-stilbene using the parent hexaruthenium cluster occurs under mild conditions [89]. PCy_3 reacts with the face-bridged clusters $Ru_3(CO)_9(\mu\text{-}H)(\mu_3\text{-}ampy)$ and $[Ru_3(CO)_9(\mu\text{-}H)_2(\mu_3\text{-}ampy)]^-$ to afford the corresponding monosubstituted PCy_3 derivatives. The neutral PCy_3-substituted cluster is a catalyst precursor for the homogeneous hydrogenation of diphenylacetylene. The synthesis and characterization (IR and NMR) of the alkenyl-bridged clusters $Ru_3(CO)_7(PCy_3)(\mu_3\text{-}ampy)(\mu\text{-}PhC{=}CHPh)$ and $Ru_3(CO)_6(PCy_3)(\mu\text{-}H)_2(\mu_3\text{-}ampy)(\mu\text{-}PhC{=}CHPh)$ are described. The X-ray structure of the former alkenyl-bridged cluster has been solved. The results of this paper are compared with those obtained for the related PPh_3-substituted clusters [90]. The synthesis, structure, and hydrogenation activity of $Ru_3(\mu_3\text{-}\eta^2\text{-}ampy)(\mu,\eta^1{:}\eta^2\text{-}PhC{=}CHPh)(CO)_6(PPh_3)_2$ have been published. The deactivation of

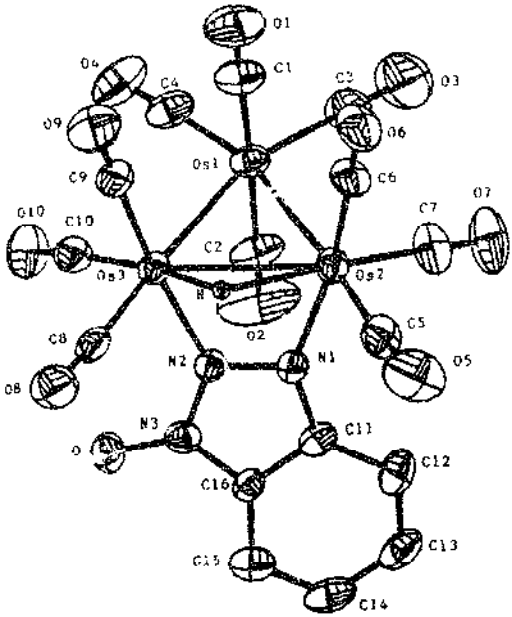

Fig. 8. Structure of one of the three clusters $Os_3(CO)_{10}[\mu_3(2,3\text{-}\eta^1)\text{-NNN(OC}_2H_4)](\mu_3\text{-}\eta^1\text{-C}^{\cdot}\text{-NHR})$. Reprinted with permission from Organometallics. Copyright 1994 American Chemical Society.

the catalyst precursor was fully explored [91]. Clusters as homogeneous catalysts in the hydrogenation of diphenylacetylene have been investigated. The cluster $Ru_3(CO)_8(\mu_3\text{-ampy})(\mu\text{-}\eta^1\text{:}\eta^2\text{-PhC=CHPh})$ promotes the hydrogenation reaction under mild conditions and without the spectroscopic observation of other ruthenium species. This sum cluster reacts with $HBF_4\cdot OEt_2$ to give $[Ru_3(CO)_8(\mu\text{-H})(\mu_3\text{-ampy})(\mu\text{-}\eta^1\text{:}\eta^2\text{-PhC=CHPh})]^+$, the X-ray structure of which is shown in Fig. 9. Reaction of this cationic cluster with $[PPN][BH_4]$ gives *cis*- and *trans*-stilbene, along with a coordinatively unsaturated cluster, which reacts with added diphenylacetylene to regenerate the neutral parent cluster. The kinetics and mechanism for the hydrogenation reaction are fully discussed [92].

$Ru_3(CO)_{12}$ reacts with 4-tert-butyl-4-methyl-1-(phenylthio)cyclobutene to furnish the new clusters $Ru_4(CO)_{12}[\mu_4\text{-}SC_2CH_2C(Me)Bu^t]$, $Ru_3(CO)_8[\{\mu_3\text{-}\eta^2\text{-}C_2CH_2C(Me)Bu^t\}(\mu_4\text{-}S)]_2$, $Ru_4(CO)_{11}[\mu_4\text{-}\eta^2\text{-}C_2CH_2C(Me)Bu^t](\mu_4\text{-}S)$, and $Ru_6(CO)_{16}[\mu_4\text{-}C^{\cdot}CH=C(Me)Bu^t](\mu_4\text{-}S)$, all of which were structurally characterized by X-ray crystallography. The coordination mode of the cyclobutene ligand and its conversion into a quadruply bridging cyclobutyne ligand are discussed [93]. 1-Bromocyclobutene activation by $Os_3(CO)_{10}(MeCN)_2$ at room temperature yields

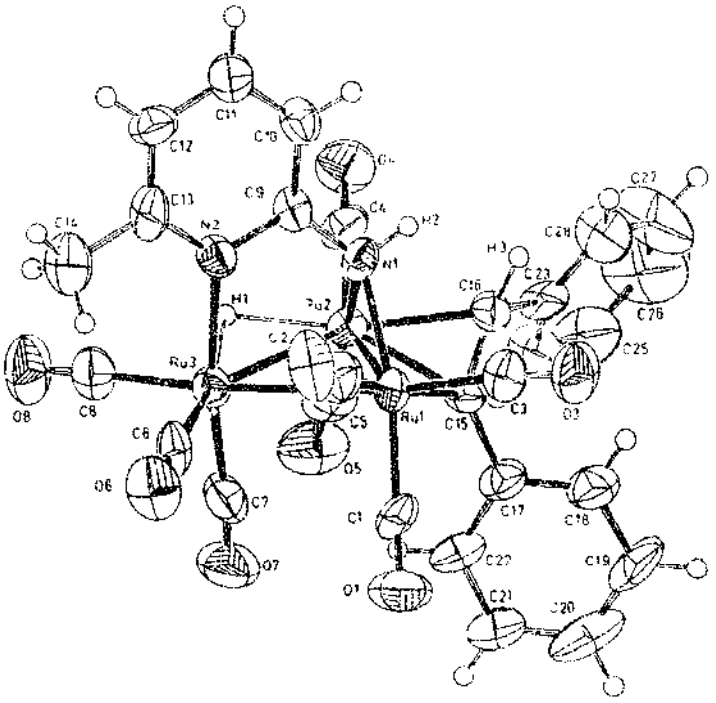

Fig. 9. Structure of $[Ru_3(CO)_8(\mu\text{-}H)(\mu_3\text{-ampy})(\mu\text{-}\eta^3,\eta^2\text{-PhC}{=}CHPh)]^-$. Reprinted with permission from Organometallics. Copyright 1994 American Chemical Society.

$Os_3(CO)_{10}(\mu\text{-Br})(\mu\text{-CCHCH}_2CH_2)$ and $Os_3(CO)_9(\mu\text{-Br})(\mu_3\text{-}\overline{CCHCH_2}\overline{CH_2})$ as the major and minor products, respectively. The former cluster contains bridging σ,π-coordinated cyclobutenyl and bromide ligands across the open Os–Os bond. This same cluster transforms into the latter cluster upon thermolysis or optical excitation. Me_3NO-induced decarbonylation of the major product also furnishes the minor product along with the new cluster $Os_3(CO)_9(\mu\text{-Br})(\mu_3\text{-}\eta^2\text{-}\overline{C_2CH_2}\overline{CH_2})(\mu\text{-H})$. All three of these clusters have been characterized by X-ray crystallography [94]. The molecular and electronic structures of the tetraruthenium clusters $Ru_4(CO)_{13}(\mu\text{-}PR_2)_2$ (where R = Ph, Pr^i, OEt, NPr^i_2, Cy, Et), which were synthesized from $[Ru_4(CO)_{13}]^{2-}$ and R_2PCl, are discussed. These phosphido-bridged clusters possess planar butterfly polyhedra with two normal and three elongated Ru–Ru bonds. All products have been characterized in solution by IR and NMR (^1H, ^{31}P, ^{13}C) spectroscopy and by X-ray crystallography in the case of the first four clusters. The electronic effects exerted on the cluster polyhedron by the two phosphido groups were examined

by extended Hückel calculations [95]. Decarbonylation of $Ru_4(CO)_{13}(\mu_3\text{-}PNPr^i_2)$ produces $Ru_4(CO)_{11}(\mu_3\text{-}PNPr^i_2)$, which upon treatment with silica gel gives $[Ru_4(CO)_{12}(\mu_3\text{-}PO)\{\eta^1\text{-}H_2NPr^i_2\}]$, as a result of aminophosphinidene ligand hydrolysis. The X-ray structures of the latter two clusters accompany this report [96]. Treatment of the 62-electron nido cluster $Ru_4(CO)_{12}(\mu\text{-}H)_4(\mu_3\text{-}PPh)$ with diphenylbutadiyne yields $Ru_4(CO)_{12}[\mu_4\text{-}\eta^1{:}\eta^1{:}\eta^1{:}\eta^3\text{-}P(Ph)C{:}C(H)Ph\}CC(H)Ph]$, $Ru_4(CO)_{10}(\mu\text{-}CO)(\mu_3\text{-}PPh)[\mu_4\text{-}\eta^1{:}\eta^1{:}\eta^1{:}\eta^2\text{-}PhC(H)CCC(H)Ph]$, and $Ru_4(CO)_{11}(\mu_3\text{-}PPh)[\mu_4\text{-}\mu^1{:}\mu^1{:}\mu^2{:}\eta^3\text{-}PhC(H)C(H)CCPh]$, which contain *trans*-diphenylbutatriene and *trans*-diphenylbut-3-en-1-yne ligands. Reaction of the last cluster with additional diyne leads to an ene–yne coupling on the Ru_4 square face and formation of $Ru_4(CO)_{10}(\mu_4\text{-}PPh)[\mu_4\text{-}\eta^1{:}\eta^1{:}\eta^1{:}\eta^3\text{-}PhCCC(H)C(H)PhC(Ph)CCCPh]$. All four products have been fully characterized, with Fig. 10 showing the crystal structure of the last cluster [97].

The tetraruthenium chain cluster $Ru_4(\mu\text{-}Br)_2[\mu\text{-}C, P{:}P\text{-}(C_6H_4)PPhCH_2PPh_2]_2(\mu\text{-}CO)(CO)_8$ has been isolated as a minor product from the reaction between $Ru_3(\mu\text{-}dppm)(CO)_{10}$ and the benzyl halides $C_6X_5CH_2Br$ (where X = H, Me, F) [98]. The ruthenium cluster $Ru_4(CO)_8(AcO)_4(PBu^t_2)_2$ was the subject of a paper dealing olefin hydroformylation. The results of hydroformylation reactions using other ruthenium carboxylate complexes are presented [99]. The redox chemistry of the nitrido cluster $[Fe_4N(CO)_{12}]^-$ has been investigated. EPR data on the dianion $[Fe_4N(CO)_{12}]^{2-}$ in frozen solution indicate that two different clusters in equilibrium are present. Phosphine substitution by an ETC route is observed when the dianion is electrochemically or chemically generated. The X-ray structure of $[Fe_4N(CO)_{11}(PPh_3)]^-$ has been solved [100]. A report on the use of $[Cp_2Fe_2(CO)_4]$-$[CN(CH_2)_nNC]$ (where $n = 2,3$) as a chelating ligand has appeared [101]. Cyclohexa-1,3-diene reacts with $Os_3(\mu\text{-}H)_2(CO)_{12}$ to give $Os_3(\mu\text{-}H)_2(CO)_{11}(\eta^2\text{-}C_6H_6)$, $Os_3(\mu\text{-}H)_2(CO)_{12}(\eta^2\text{-}C_6H_8)$, $Os_3(\mu\text{-}H)_2(CO)_{11}(\eta^4\text{-}C_6H_8)$,

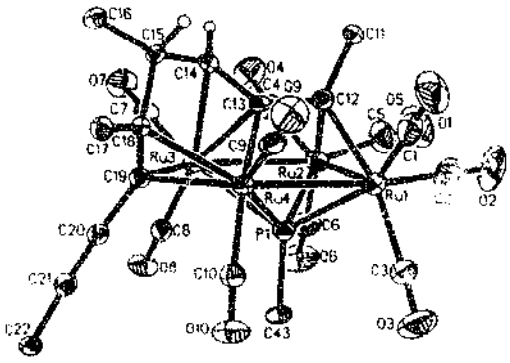

Fig. 10. Structure of $Ru_4(CO)_{10}(\mu_4\text{-}PPh)[\mu_4\text{-}\eta^1{:}\eta^1{:}\eta^1{:}\eta^3\text{-}PhCCC(H)C(H)PhC(Ph)(CCPh)]$. Reprinted with permission from Organometallics. Copyright 1994 American Chemical Society.

and $Os_4(\mu\text{-}H)_2(CO)_{10}(\eta^6\text{-}C_6H_6)$ as the major products. The last cluster also undergoes further reaction with cyclohexa-1,3-diene to afford $Os_4(CO)_8(\eta^6\text{-}C_6H_6)(\eta^4\text{-}C_6H_8)$ and $Os_4(\mu\text{-}H)_2(CO)_8(\eta^6\text{-}C_6H_6)(\eta^4\text{-}C_6H_8)$. Schemes illustrating the reactivity relationship between these clusters have been presented [102]. Low-pressure hydrogenation of $Ru_2(\eta^6\text{-}C_6H_6)_2Cl_4$ in water containing $NaClO_4$ gives the oxo-capped trinuclear cluster $[Ru_3(\eta^6\text{-}C_6H_6)_3(\mu\text{-}CH)(\mu_3\text{-}O)(\mu\text{-}H)]^+$. Starting with the durene derivative and using high hydrogen pressure (60 atm) leads to the chloro-capped cluster $[Ru_3(\eta^6\text{-}C_6H_2Me_4)_3(\mu_3\text{-}CH)H_3]^{2+}$, which undergoes hydrolysis to give the corresponding oxo-capped cluster. The tetranuclear cluster $[Ru_4(\eta^6\text{-}C_6H_6)_4H_4]^{2+}$ has been isolated from the hydrolysis of $Ru_2(\eta^6\text{-}C_6H_6)_2Cl_4$ in the presence of H_2 [103]. Photolysis of $Ru_3(CO)_9BH_5$ in MeCN and $M(CO)_6$ (where M is Cr, Mo, W) furnishes the ruthenaborane cluster $Ru_4H(CO)_{12}BH(\mu\text{-}NCHMe)$, the X-ray structure of which exhibits a butterfly polyhedron with a semi-interstitial boron atom. The bonding in this cluster has been examined by Fenske–Hall calculations, with the data supporting a model of localized bonding in the region of the B–N–Ru bridge, as required for a 62-electron cluster [104]. Refluxing a mixture of $Cp^*_2Fe_2(CO)_4$, sulfur, and diphenylacetylene affords the tetrairon clusters $Cp^*_2(Ph_2C_2S_2)_2Fe_4S_4$ and $Cp^*_2(Ph_2C_2S_2)Fe_4S_4$. The use of other alkynes leads to analogous clusters. The X-ray structures of the two diphenylacetylene clusters are included in this report (Fig. 11) [105].

Reductive carbonylation of ∞-$[Os(CO)_3Cl_2]_2$ or $OsCl_3$ supported on SiO_2 in the presence of K_2CO_3 leads to high yields of $[Os_4(CO)_{13}H_3][K]$. The use of surface-mediated syntheses versus traditional solution methods is stressed [106]. Variable-

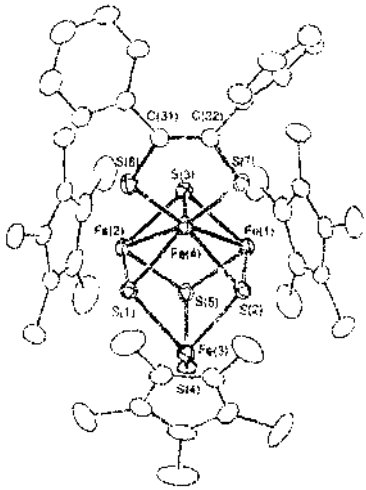

Fig. 11. Structure of $Cp^*_2(Ph_2C_2S_2)_2Fe_4S_4$. Reprinted with permission from Inorganic Chemistry. Copyright 1994 American Chemical Society.

temperature solution and solid-state NMR measurements on $Ru_4H_4(CO)_{12}$ have been carried out, and the data are discussed in terms of dynamic hydride behavior. The carbonyl polyhedron is rigid based on the ^{13}C chemical shift tensor components [107]. Thermolysis of $Cp^*Os_4(\mu\text{-}H)(CO)_{12}$ at 50 C results in the loss of CO and production of $Cp^*Os_4(\mu\text{-}H)(CO)_{11}$. Thermolysis of this latter cluster at 90 C gives the clusters $[\mu,\eta^5,\eta^1\text{-}C_5Me_4CH_2]Os_4(\mu\text{-}H)_2(CO)_{10}$, $[\mu,\eta^5,\eta^1\text{-}C_5Me_4CH_2]Os_4(CO)_{11}$, and $[\mu,\eta^5,\eta^1\text{-}C_5Me_3(CH_2)_2]Os_4(\mu\text{-}H)_2(CO)_9$. Each of these tetrahedral clusters has been structurally characterized by X-ray crystallography (Fig. 12), and schemes that show the stepwise C–H bond activation and the relationship between these clusters are discussed [108].

The kinetics for CO substitution in the carbide cluster $Ru_5C(CO)_{15}$ have been examined with twenty-one different phosphine/phosphite ligands. For ligands with cone angles less than 133°, a two-step reaction is observed, where the intermediate cluster $Ru_5C(CO)_{14}L$ is shown to lose CO in the subsequent step to give the corresponding monosubstituted cluster. Larger cone angle ligands react with $Ru_5C(CO)_{15}$ in a bimolecular reaction with no spectroscopic evidence for adduct formation. Reaction mechanisms, transition-state flexibility, and quantitative data on the dependence of the observed rate constants on the electronic and steric properties of the P-ligands are presented [109]. The electron-rich vinylidene clusters $Ru_5(\mu_5\text{-}CCHR)(\mu_3\text{-}SMe)_2(\mu\text{-}PPh_2)_2(CO)_{10}$ have been isolated from the reaction of $Ru_5(\mu_5\text{-}C_2)(\mu\text{-}SMe)_2(\mu\text{-}PPh_2)_2(CO)_{11}$ with hydrogen and alkenes. X-ray structures of two of the products reveal that the Ru_5 core consists of three edge-sharing triangles. These 80-electron clusters have elongated Ru–Ru bonds owing to the occupation of Ru–Ru antibonding orbitals [110]. The kinetics for benzene migration from a μ_3-

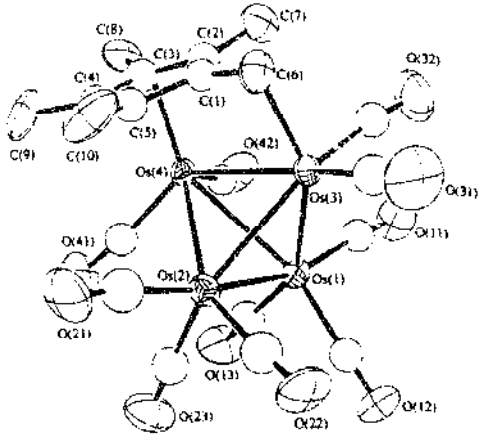

Fig. 12. Structure of $[\mu,\eta^5,\eta^1\text{-}C_5Me_4CH_2]Os_4(\mu\text{-}H)_2(CO)_{11}$. Reprinted with permission from Organometallics. Copyright 1994 American Chemical Society.

η^2:η^2:η^2 position to an η^6 site in $Ru_5C(CO)_{12}(C_6H_6)$ have been measured by ^1H NMR spectroscopy. A working mechanism for this isomerization is presented, and the data are discussed relative to benzene surface phenomena on closed-packed metal surfaces [111]. The synthesis and X-ray structure of $[(Me_2SiCp_2)_2Fe_5(\mu_3\text{-}S_2)_2(\mu_4\text{-}S_2)][FeCl_4]$ have been published [112]. The cyclic voltammetric behavior of $Cp^*_2(Ph_2C_2S_2)_2Fe_4S_4$ reveals the presence of four reversible one-electron redox waves. The structural changes associated with each redox process are discussed, and the X-ray structures of several clusters are presented [113]. Treatment of $Ru_5C(CO)_{15}$ with cyclohexa-1,3-diene in the presence of Me_3NO affords the clusters $Ru_5C(CO)_{11}(\eta^4\text{-}C_6H_8)_2$, $Ru_5C(CO)_{12}(\mu_5\text{-}\eta^2\text{:}\eta^2\text{:}\eta^2\text{-}C_6H_6)$, and $Ru_5C(CO)_{12}(\eta^6\text{-}C_6H_6)$. The X-ray structure of the first product cluster has been solved, revealing the existence of terminally bound cyclohexadiene ligands on opposite basal ruthenium atoms of the square-pyramidal ruthenium polyhedron [114]. The bonding in the arene-substituted clusters $Ru_5C(CO)_{12}(C_6H_6)$ and $Ru_6C(CO)_{11}(C_6H_6)$ has been studied by extended Hückel calculations, with attention paid to the bonding mode exhibited by the arene ligand [115]. Addition of $Os(CO)_4(CNBu^t)$ to $Os_4(CO)_{14}$ leads to $Os_5(CO)_{18}(CNBu^t)$, which possesses a bow-tie arrangement of osmium atoms, as determined by X-ray crystallography. The isonitrile ligand occupies an axial site on an outer osmium atom. Thermolysis of this cluster at ambient temperature gives $Os_5(CO)_{17}(CNBu^t)$, which is suggested to have a raft configuration of osmium atoms. Loss of two CO groups from $Os_5(CO)_{17}(CNBu^t)$ furnishes $Os_5(CO)_{15}(CNBu^t)$, the molecular polyhedron of which is based on a distorted trigonal bipyramidal geometry. The site preference of the isonitrile ligand in these clusters is controlled by electronic rather than steric effects [116]. Treatment of $Ru_5C(CO)_{15}$ with 1,5,9-trithiacyclododecane (12S3) in refluxing hexane gives $Ru_5C(CO)_{13}(\mu\text{-}\eta^1\text{-}12S3)$ in high yield. When the same reaction is conducted in boiling octane, the new cluster $Ru_5C(CO)_{11}(\mu\text{-}\eta^3\text{-}12S3)$ was formed as the major product. Independent experiments show that the cluster $Ru_5C(CO)_{13}(\mu\text{-}\eta^1\text{-}12S3)$ transforms into $Ru_5C(CO)_{11}(\mu\text{-}\eta^3\text{-}12S3)$. Both sulfur-bridged clusters were characterized in solution and by X-ray crystallography (Fig. 13) [117].

The deprotonation and subsequent auration of the hexanuclear raft cluster $Ru_6(\mu_4\text{-}H)(\mu\text{-}H)(\mu\text{-}O)\mu\text{-}C\text{:}\eta^6\text{-}OC_6H_3OMe\text{-}4)(CO)_{16}$ are reported. The molecular structure of the product formed in each of these reactions has been established by X-ray analysis [118]. The dianion $[Os_5(CO)_{15}]^{2-}$ reacts with $[Os(\eta^6\text{-}C_6H_6)(MeCN)_3]^{2+}$ and $Os(C_6H_5Me)(OTf)_2$ to give $Os_6(CO)_{15}(\eta^6\text{-}C_6H_6)$ and $Os_6(CO)_{15}(\eta^6\text{-}C_6H_5Me)$, respectively. Chemical reduction of $Os_6(CO)_{18}$ using K-Ph_2CO affords the dianion $[Os_6(CO)_{17}]^{2-}$ in quantitative yield, which was subsequently examined as a reagent in the synthesis of $Os_6(CO)_{15}(\eta^6\text{-}C_6H_6)$. This report discusses the X-ray data of several high-nuclearity osmium clusters [119]. Treatment of $[Fe_3(CO)_9CCO]^{2-}$ with triflic anhydride leads to the transient cluster $[Fe_3(CO)_9C_2]$, followed by carbon–carbon coupling of the carbide ligands and formation of $[Fe_6(CO)_{18}C_2]^{2-}$. The presence of the C_2 moiety in this cluster was ascertained by X-ray crystallography [120]. The catalytic activity of the carbide cluster $[Ru_6C(CO)_{16}Me][PPN]$ in alkene hydrogenation reactions has been explored. The clusters $[Ru_6C(CO)_{16}H][PPN]$ and $[Ru_6C(CO)_{15}H][PPN]$ have

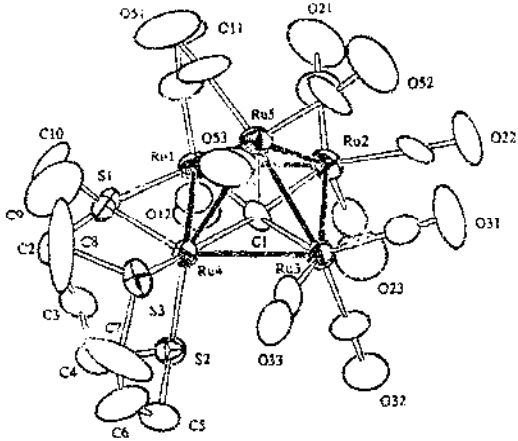

Fig. 13. Structure of $Ru_6C(CO)_{12}(\mu$-η^3-12S2). Reprinted with permission from Organometallics. Copyright 1994 American Chemical Society.

been isolated from these reactions, and the X-ray structure of each cluster discussed [121]. The synthesis and structural characterization of $Ru_6C(CO)_{12}Cp_2$ and $Ru_5C(CO)_{10}Cp_2$ have been published [122]. The molecular structure of $Ru_6C(CO)_{11}(\eta^6$-$C_6H_4Me_2)_2$ has been solved by X-ray crystallography (Fig. 14). Chemical aspects of heteromolecular crystals of this cluster and $Ru_6C(CO)_{14}(\eta^6$-$C_6H_4Me_2)$ are discussed with respect to packing efficiency and crystal cohesion [123].

The use of $[Te_6Fe_8(CO)_{24}]^{2-}$ as a starting material for the diiron complexes $Fe_2(CO)_6[\mu$-$Fe(CH_2)_nTe]$ (where $n = 1, 2, 3$) is reported [124]. Vacuum pyrolysis of $Os_3(CO)_{10}(MeCN)_2$ at temperatures above 260 °C produces the dianions $[Os_{17}(CO)_{36}]^{2-}$ and $[Os_{20}(CO)_{40}]^{2-}$, which have been characterized by X-ray crystallography and ^{13}C NMR spectroscopy. These two clusters are the largest osmium carbonyl clusters isolated to date [125]. The build-up of osmium clusters by rafting from the triangle to the octahedron has been discussed by using metal cluster topology [126]. The high-nuclearity ruthenium clusters $Ru_6(CO)_{11}(PBu^t)_3$, $Ru_7(CO)_{14}(PBu^t)_3$, and $H_3Ru_6(CO)_{20}(\mu_3$-$P)(PBu^t)_3$ have been isolated from the thermolysis reaction of $Ru_3(CO)_{12}$ and $P_2Bu^t_4$. All three of these clusters have been structurally characterized by X-ray crystallography, with the latter cluster being the first example of a cluster possessing a semi-encapsulated μ_3-P moiety [127]. The relationship between the geometric and electronic structure of Fe_4B_2 clusters has been investigated by using Fenske Hall molecular orbital calculations. Related dodecahedral cobalt and nickel clusters were also studied [128]. The reaction of $[Fe_4(CO)_{12}HB]^{2-}$ with either $Fe_2(CO)_9$ or $Fe(CO)_3$(*cis*-cyclooctene)$_2$ leads to the sequential formation of $[HFe_5(CO)_{15}B]^{2-}$, $[HFe_6(CO)_{17}B]^{2-}$, and $[HFe_7(CO)_{20}B]^{2-}$. It is suggested that the cluster building sequence is initiated by

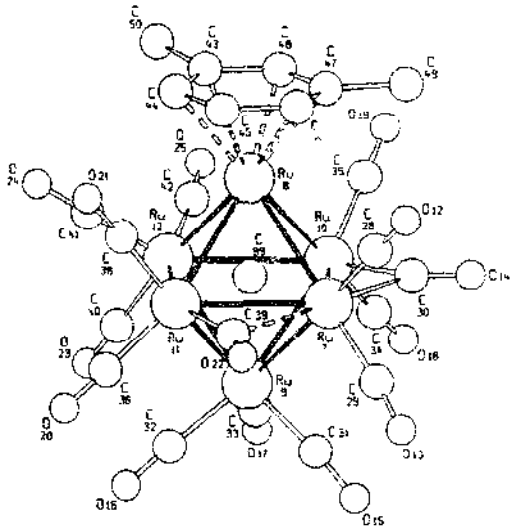

Fig. 14. Structure of $Ru_4C(CO)_{11}(\eta^6\text{-}C_6H_2Me_4)$. Reprinted with permission from Organometallics. Copyright 1994 American Chemical Society.

electron transfer from $[Fe_4(CO)_{13}HB]^-$ to $Fe_3(CO)_{12}$, which gives $Fe(CO)_5$ as a byproduct. The solid-state structure of the heptairon cluster has been established (Fig. 15) [129].

2.5. *Group 9 clusters*

A report describing the X-ray structure of $Co_3Cp_3(\mu_3\text{-}S)(\mu_3\text{-}CNC_6H_2Me_4)$ has been published [130]. The electronic structures of the tricobalt clusters $Co_3(\mu_3\text{-}X)(\mu\text{-}CO)_3(PMe_3)_3$ (where X is H, Cl, Br, I) have been explored by INDO/2 and/or QR-INDO/1 calculations [131]. Treatment of cobaltous salts with *o*-mercaptophenolate ligands (mp^{2-}) and trialkylphosphines yields trinuclear and tetranuclear complexes, the magnetic susceptibility properties of which indicate the existence of antiferromagnetic behavior [132].

1-Pentene hydroformylation using $PhCCo_3(CO)_9$ has been studied by cylindrical internal reflectance (CIR) spectroscopy. Aldehyde formation is shown to coincide with cluster fragmentation, suggesting mononuclear catalysis. These data are discussed with respect to other reactions employing $PhCCo_3(CO)_9$ as a catalyst precursor [133]. CIR spectroscopy of the hydroformylation of 1-pentene using $PhCCo_3(CO)_7[(Z)\text{-}Ph_2PCH{=}CHPPh_2]$ reveals the presence of extensive cluster fragmentation to $[Co(CO)_4]^-$ in the early stages of the reaction [134]. The reaction

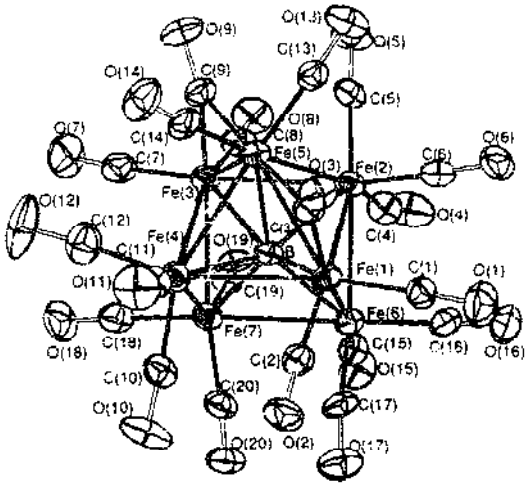

Fig. 15. Structure of $[HFe_4(CO)_{13}B]^-$. Reprinted with permission from Inorganic Chemistry. Copyright 1994 American Chemical Society.

of $HCCo_3(CO)_9$ with Ph_nSiH_{4-n} and $HR_2SiXSiR_2H$ has been investigated. The clusters $HMe_2SiXSiMe_2CCo_3(CO)_9$ and $(OC)_9Co_3CMe_2SiXSiMe_2CCo_3(CO)_9$ (where X is O, 1,4-C_6H_4) have been isolated and characterized in solution. Cluster coupling reactivity with $RSiH_3CCo_3(CO)_9$ (where R is Ph, Me) or sterically demanding silanes is not observed. Use of Ph_nSiH_{4-n} (where $n=1, 2$) leads to electrophilic attack on the cluster core, giving the μ-silylene clusters $HCCo_3(CO)_8(\mu\text{-}SiR_2)$, which have been characterized in solution. No electronic interactions were observed between the Co_3 cores of these dicluster compounds, as judged by electrochemical measurements [135]. The gas-phase chemistry of the radical anions of the capped-cobalt clusters $XCCo_3(CO)_9$ (where X is H, Me, Ph, CO_2Me, F, Cl) has been examined by tandem mass spectrometry (MS/MS) and Fourier transform mass spectrometry (FTMS). The molecular anions are not stable, giving $XCCo_3(CO)_n^-$ fragments by CO loss via dissociative electron capture [136]. The use of water-soluble ligands $[PPh_{3-n}(C_6H_4SO_3-m)_n]^{n-}$ (where $n=1,3$) in the preparation of the water-soluble clusters $[RCCo_3(CO)_8P]^{n-}$ (where R is Ph, Me, Cl, Br) is described. The electrochemical behavior of these clusters was examined by cyclic voltammetry in water. The ability of the sulfonated ligand to influence the kinetic parameters of the CV experiment is discussed [137]. Photolysis of $CpCo(CO)_2$ in toluene gives $Cp_3Co_3(\mu_2\text{-}CO)_2(\mu_3\text{-}CO)$ and the new all-bridging isomer $Cp_3Co_3(\mu_2\text{-}CO)_3$, the molecular structure of which was established by X-ray crystallography (Fig. 16). The redox properties of this new isomer were explored and found to be different from the known $Cp_3Co_3(\mu_2\text{-}CO)_3(\mu_3\text{-}CO)$ and $Cp_3Co_3(\mu_2\text{-}CO)_2(CO)$ isomers [138].

The synthesis and thermal decomposition of $Cp_2Co_4(CO)_{5-n}(PPh_2H)$(alkyne)

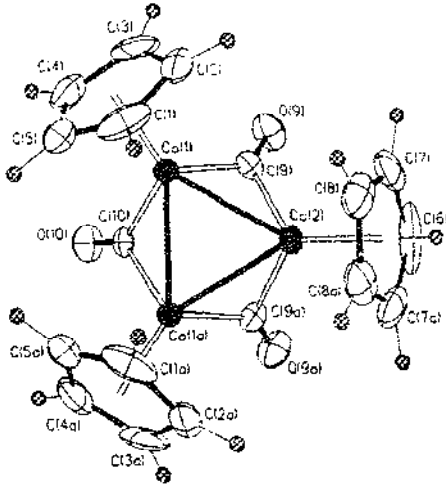

Fig. 16. Structure of $Cp_3Co_3(\mu_3\text{-}CO)_3$. Reprinted with permission from Inorganic Chemistry. Copyright 1994 American Chemical Society.

have been reported [139]. Thermolysis of a 1:1 mixture of $(\eta^5$-indenyl$)Ir(CO)_2$ and $(\eta^5$-indenyl$)Ir(ethylene)_2$ gives the triiridium cluster $(\eta^5$-indenyl$)_3Ir_3(\mu\text{-}CO)_3$. The molecular structure shows idealized C_{3v} symmetry and consists of a triangular array of iridium atoms and edge-bridging CO groups. The reaction between $(\eta^5$-indenyl$)Ir(CO)_2$ and $(\eta^5$-indenyl$)Rh(ethylene)_2$ affords all of the possible trinuclear products [140]. Site-selective oxidation addition of a variety of electrophiles in the clusters $Ir_3(\mu\text{-}PPh_2)_3(CO)_3(dppm)$ and $Ir_3(\mu\text{-}PPh_2)_3(CO)_4(CNBu^t)_3$ occurs at the formally 16-electron iridium center in each cluster. All of the products have been fully characterized in solution and by X-ray crystallography in the case of two clusters [141]. The X-ray structures of $Cp^*_3Co_3(\mu_3\text{-}CCH_3)_2$ and $Cp^*_3Co_3(\mu_3\text{-}CCH_3)(\mu_3\text{-}H)$, which were obtained from the reaction between acetylene and $Cp^*Co(ethylene)_2$, have been solved [142]. Ligand addition in the cluster $Cp^*_3Co_3(\mu_3\text{-}CCH_3)(\mu_3\text{-}H)$ by CO and $CNBu^t$ gives $Cp^*_3Co_3(\mu_3\text{-}CCH_3)(\mu_3\text{-}CO)(\mu_2\text{-}H)$ and $Cp^*_3Co_3(\mu_3\text{-}CNBu^t)(\mu_2\text{-}H)$, respectively. Use of NO leads to the face-bridged nitrosyl cluster $Cp^*_3Co_3(\mu_3\text{-}CCH_3)(\mu_3\text{-}NO)$. All three of these addition products have been characterized in solution and by X-ray crystallography. Variable-temperature NMR data on the CO- and isonitrile-bridged clusters have allowed the barrier for hydride migration about these clusters to be calculated [143]. The paramagnetic cluster $Cp^*_3Co_3(\mu_2\text{-}H)_3(\mu_3\text{-}H)$ reacts with CO (2 equiv.) to form the 48-electron cluster $Cp^*_3Co_3(\mu_2\text{-}CO)(\mu_3\text{-}CO)(\mu\text{-}H)_2$, the X-ray structure of which shows an equilateral triangle of cobalt atoms with bridging CO and hydride ligands. The fluxional behavior of the two CO ligands has been studied by ^{13}C NMR line-

shape analysis, which gives the activation parameters for CO interconversion between the μ_2- and μ_3-CO coordination modes. This same cluster loses H_2 at elevated temperature to give $Cp^*_3Co_3(\mu_3\text{-}CO)_2$. Treatment of the starting tetrahydride cluster with $CNBu^t$ at low temperature gives $Cp^*_3Co_3(\mu\text{-}CNBu^t)_2(\mu\text{-}H)_2$, followed by isonitrile insertion into a Co–H bond to yield the formimidoyl cluster $Cp^*_3Co_3(\mu_3\text{-}\eta^2\text{-}CH(=NBu^t))(\mu\text{-}H)$ upon warming. The X-ray structure of the formimidoyl cluster is shown in Fig. 17. Schemes showing the coordination and transformation chemistry of ligands in these tricobalt clusters are presented [144].

The solid-state structures and the pathways available for metal and carbonyl scrambling in $M_4(CO)_{12}$ and $M_4(CO)_{12-n}L_n$ (where M is Co, Rh, Ir; $n = 1$–5) have been examined [145]. $Ir_4(CO)_{12}$ undergoes a base-induced condensation reaction to yield $[Ir_6(CO)_{20}]^{2-}$ and $[Ir_8H_1(CO)_{22}]^{4-}$. Oxidation of the trianionic cluster gives the decairidium cluster $[Ir_{10}(CO)_{30}]^{2-}$. The X-ray structures of the iridium hydride and the decairidium clusters are presented, and the build-up process of closed-shell trigonal-pyramidal polyhedra discussed [146]. The reaction of $[Cp^*CoCl]_2$ with $LiBH_4$ leads to the polynuclear compounds *closo*-2,3,4-$(Cp^*Co)_3B_2H_4$, *closo*-1,2,3-$(Cp^*Co)_3B_3H_5$, and *closo*-1,2,3,6-$(Cp^*Co)_4B_2H_4$ via the intermediates $[Cp^*Co(BH_3)]_x$ and $(Cp^*Co)_2B_2H_6$ [147]. The dinuclear compounds $[Cp^*MCl_2]_2$ (where M is Rh, Ir) react with $E(SiMe_3)_2$ (where E is Se, Te) to give the cubane clusters $[Cp^*ME]_4$. The X-ray structures of the four possible M/E cubane clusters are presented [148]. Polynuclear rhodium(II) compounds possessing phosphinophenoxide ligands have been synthesized [149]. Use of $Rh_4(CO)_{12}$ as a catalyst precursor in the homogeneous water-gas shift reaction is reported. The cluster $[Rh_3(CO)_{13}(py)_2]^-$ was found to accumulate during the catalysis using pyridine as the base. The reactivity of this anionic cluster and its role in the water-gas shift reaction are discussed [150]. The cubane cluster $[Cp^*IrS]_4$ has been isolated from $Cp^*Ir(PMe_3)S_2IrCp^*$ and structurally characterized. The results of kinetic studies are presented, and a working mechanism for the formation of $[Cp^*IrS]_4$ outlined

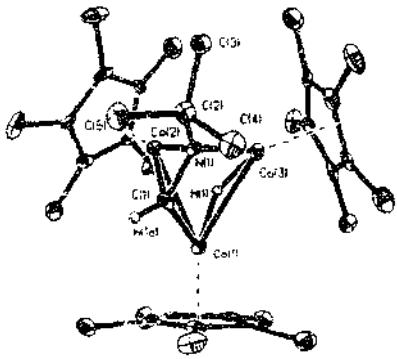

Fig. 17. Structure of $Cp^*_3Co_3(\mu_3\text{-}\eta^2\text{-}CH(=NBu^t))(\mu\text{-}H)$. Reprinted with permission from Organometallics. Copyright 1994 American Chemical Society.

[151]. The X-ray structure of $[\{Cp^*_2Rh_2(\mu_3\text{-}CH_2)_2\}_2(\mu_4\text{-}S)]^{2+}$, which derives from the stepwise abstraction of the [SH]$^-$ ligand from a dirhodium dihydrosulfide compound by $[Ag]^+$ ions, is reported [152]. Surface-mediated synthesis of $[Rh_5(CO)_{15}]^-$ and $[Rh_{12}(CO)_{30}]^{2-}$ from chemisorbed $Rh(CO)_2(acac)$ and CO is described. The supports used in this study were MgO and $\gamma\text{-}Al_2O_3$ [153]. Reaction of PPh_3 with $[Rh_6C(CO)_{16}]^{2-}$ yields the first reported carbide-substituted rhodium cluster with a trigonal-prismatic structure. This cluster loses CO to give the octahedral cluster $[Rh_6C(CO)_{12}]^{2-}$, as shown by X-ray crystallography [154]. The nitrido cluster $[Rh_6N(CO)_{15}]^-$ reacts with metal hydroxides in water or alcohol solutions to give the hydride cluster $[Rh_6(\mu\text{-}H)N(CO)_{14}]^{2-}$, which has been characterized in solution and by X-ray crystallography. The solid-state structure contains a trigonal-prismatic core with a central nitrido ligand [155]. The ligand substitution chemistry of $Rh_6(CO)_{16}$ using Me_3NO activation has been published. The solution and solid-state structures of the isolated $Rh_6(CO)_{14}L_2$ clusters (where L is MeCN, py, $P(OPh)_3$) have been established by NMR spectroscopy and X-ray crystallography [156]. A paper on the mathematical modeling of ligand arrangements in various octahedral clusters has appeared [157].

2.6. Group 10 clusters

Treatment of the hydroxo complex $[Ni_3(C_6F_5)_4(\mu\text{-}OH)_2]^{2-}$ with EtSH leads to the formation of the trinuclear cluster $[Ni_3(C_6F_5)_4(\mu\text{-}SEt)_2]$, the X-ray structure of which accompanies this report [158]. Xylyl isonitrile reacts with $[Pd_3(\mu_3\text{-}CO)_2(\mu\text{-}dppm)_3]^{2+}$ to give the binuclear complex $[Pd_2(CNC_6H_3Me_2\text{-}2,6)_2(\mu\text{-}dppm)_2]^{2+}$, along with an unidentified palladium(II) species. These same products react over time to give the new trinuclear cluster $[Pd_2(CNC_6H_3Me_2\text{-}2,6)_2\{\mu\text{-}Pd(CNC_6H_3Me_2\text{-}2,6)_2\}(\mu\text{-}dppm)]^{2+}$, which has been fully characterized in solution and by X-ray crystallography [159]. The controlled-potential electrolysis of mononuclear platinum(II) complexes $[Pt(P\text{–}P)(CNR)_2]^{2+}$ (where P–P is diphosphine) is reported to give the trinuclear platinum clusters $[\{Pt(P\text{–}P)(CNR)_2\}_3Pt]^{2+}$. These clusters, which contain a coordinatively unsaturated platinum center, have been examined for their redox properties at a mercury-pool electrode. Isolated from these electrochemical studies is a variety of platinum clusters, the composition of which is dependent on the size of the ancillary P–P ligand [160]. A report dealing with the host-guest chemistry of $[Pd_3(dppm)_3(\mu_3\text{-}CO)]^{2+}$ and many inorganic and organic substrates has appeared. The binding constants have been measured spectroscopically by using Benesi–Hilderband, Scatchard, and Scott methods. The binding strength of a substrate into the cavity composed of the metallic and hydrophobic sections is discussed relative to several parameters [161]. Evidence for excited-state host–guest chemistry with the tripalladium cluster $[Pd_3(dppm)_3(\mu_3\text{-}CO)]^{2+}$ is presented. The excited-state electronic and structural properties of the cavity are discussed, in addition to the photophysics for host–guest deactivation [162]. The X-ray structure of the triplatinum complex $Pt_3(C_6F_5)_4(\mu\text{-}C{\equiv}CPh)_4{\cdot}4THF$ has been published. The synthesis and solution characterization of related acetylide complexes accompany this report [163]. Treatment of M^{2+} (where M is Ni, Pd, Pt) with dppe and

NaSeH or NaTeH gives the clusters $[Pd_3Se_2(dppe)_3]^{2+}$, $[Pt_3Se_2(dppe)_3]^{2+}$, $[Ni_3Te_2(dppe)_3]^{2+}$, $[Pd_3Te_2(dppe)_3]^{2+}$, and $[Pt_3Te_2(dppe)_3]^{2+}$. The X-ray structure of the last cluster is presented, and the cyclic voltammetric properties of all products are reported [164]. Thermolysis of the palladium carboxylate clusters $Pd_4(CO)_4(OCOR)_4$ (where R is Me, Bu^t, Ph, CF_3, CCl_3) releases CO_2, CO, and biacyls. In aromatic solvents, the insertion of CO_2 into an aromatic C–H bond is observed. The decomposition chemistry of other palladium systems is discussed [165]. SO_2 and L (where L is 2,6-dimethylphenylisonitrile) have been allowed to react with $Pt_5(\mu\text{-}SO_2)_x(\mu\text{-}L)_3L_7$ (where $x = 0, 2, 3$), and the resulting products isolated and characterized by traditional methods [166]. The bonding in a series of cubic $M_8(\mu_4\text{-}E)_6L_n$ clusters has been analyzed by extended Hückel and self-consistent field multiple-scattering Xα calculations [167].

2.7. Group 11 clusters

A relativistic molecular orbital study on the tetragold complex $[Au_4(PBu^t_3)_4]^{2+}$ has been published [168]. Displacement of the THT ligand from $[Au_2(\mu\text{-}CH_2PPh_2CH_2)_2(R)(THT)]^+$ (where R is C_6F_5, 2,4,6-$C_6H_2F_3$) by the dithiocarbamate ion gives the tetranuclear compounds $[\{Au_2(\mu\text{-}CH_2PPh_2CH_2)_2R_2\}_2(\mu\text{-}S_2CNR'_2)]^+$ (where R′ represents various groups) [169]. Gold–gold interactions in main group $X_nA(AuPR_3)_m$ molecules have been analyzed by extended Hückel calculations [170]. Extended Hückel calculations have been carried out on Au_5 chain compounds, with the results of metal–metal bonding discussed [171]. $[Au(PPh_3)_2]^+$ reacts with the dinuclear compound $Au_2(\mu\text{-}CH_2PPh_2CH_2)_2$ to afford the trinuclear compound $[Au_3(\mu\text{-}CH_2PPh_2CH_2)_2(PPh_3)_2]^+$, the molecular structure of which has been confirmed by X-ray crystallography [172]. Cl_2 or Br_2 oxidative addition to $Au_4(C_6F_5)_2\{(Ph_2P)_2CH\}_2$ leads to $Au_4(C_6F_5)_2\{(Ph_2P)_2CH\}_2X_2$. The halide displacement reactivity in the chloro derivative by THT and phosphines has been studied [173]. The synthesis and X-ray structure of the luminescent, one-dimensional gold(I) polymer $[Au_2\{2,6\text{-bis(diphenylphosphino)pyridine}\}(C{\equiv}CPh)_2]_\infty$ are reported. The crystal structure contains repeating units of the $Au_2L(C{\equiv}CPh)_2$ moiety [174]. $Au_2[(Z)\text{-}Ph_2PCH{=}CHPPh_2]Cl_2$ reacts with Na_2mnt to produce $Au_2(mnt)[(Z)\text{-}Ph_2PCH{=}CHPPh_2]_2Cl_2$. This new complex was characterized in solution by IR and NMR spectroscopy, and the solid-state structure was determined by X-ray diffraction analysis [175]. Mixed-valent linear gold clusters have been prepared from the asymmetric gold(III) complexes $RAu(CH_2PPh_2CH_2)_2AuX$ (where R is C_6F_5, 2,4,6-$C_6H_2F_3$; X is halogen). The treatment of these starting materials with $AgClO_4$, followed by the addition of $[AuR_2]^-$, leads to the pentanuclear $[\{RAu(CH_2PPh_2CH_2)_2Au\}_2AuR_2]^+$ or the hexanuclear $[\{RAu(CH_2PPh_2CH_2)_2Au\}_2Au(CH_2PPh_2CH_2)_2Au]^+$ compounds. The X-ray structure of the hexanuclear compound (R is $C_6H_2F_3$) is shown in Fig. 18 [176].

A report on the synthesis and characterization of copper stannyl and silyl complexes prepared from $[Ph_3PCuH]_6$ has appeared [177].

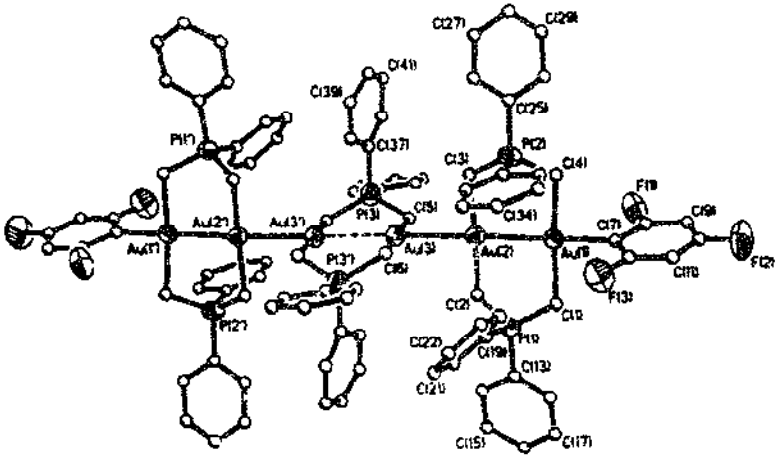

Fig. 18. Structure of $[\{RAu(CH_2PPh_2CH_2)_2Au\}_2Au(CH_2PPh_2CH_2)_2Au]^+$ (R is $C_6H_2F_3$). Reprinted with permission from Organometallics. Copyright 1994 American Chemical Society.

3. Heteronuclear clusters

3.1. Trinuclear clusters

The synthesis and NMR properties of $[(\eta^5\text{-}C_5Me_3TMS_2)_3Nb_2(\mu\text{-}H)_2H_2Au]^+$ are reported. The hydride ligands exhibit large quantum mechanical exchange couplings that have been examined as a function of temperature. The X-ray structure of this trinuclear compound accompanies this report [178].

The use of the μ-isophosphaalkyne complex $Cp_2(CO)_2(\mu\text{-}CO)Fe_2(\mu\text{-}CPMes)$ as a building block for the construction of the polynuclear compounds $Cp_2(CO)_2(\mu\text{-}CO)Fe_2[\mu\text{-}CP(M)Mes]$ (where M is $Cr(CO)_5$, $Fe(CO)_4$, $Pt(PPh_3)$ is described. Whereas the former two metals are attached to the phosphorus atom in an η^1-fashion, the $Pt(PPh_3)$ moiety is shown to bind to the μ-CP linkage and an iron atom by X-ray crystallography [179]. The antiferromagnetic clusters $Cp_2Cr_2(\mu_3\text{-}S)_2(\mu\text{-}SCMe_3)_2Re(CO)(NO)$, $CpCr(\mu\text{-}OSCMe_3)_2(\mu_3\text{-}S)Re_2(\mu\text{-}Cl)(\mu\text{-}SCMe_3)(CO)_3(NO)_2$, and $[CpCr(\mu_3\text{-}S)_2(\mu\text{-}SCMe_3)_2Re(CO)(NO)]_2$ have been prepared. The X-ray structures of several products are presented [180]. The synthesis and spectroscopic characterization of $[Ni_2(C_6F_5)_2(\mu\text{-}MS_4)]^{2-}$ (where M is Mo, W) have appeared. X-ray diffraction analysis of the tungsten derivative reveals that a central tetrahedral S_2WS_2 unit bridges two terminal square-planar $Ni(C_6F_5)$ units [181]. Treatment of $[MSe_4]^{2-}$ (where M is Mo, W) with CuCN in MeCN affords $[(NC)Cu(\mu\text{-}Se)_2M(\mu\text{-}Se)_2Cu(CN)]^{2-}$. Both compounds are shown to be isostructural. Addition of excess PMe_2Ph to these compounds leads to $[(NC)Cu(\mu\text{-}Se)_2MSe_2]^{2-}$. The X-ray structures of both molybdenum compounds are reported

[182]. The complexes $(CO)_5M{=}C(OEt)(C{\equiv}CPh)$ (where M is Cr, W) react with $Co_2(CO)_8$ to give the alkyne-ligated complexes $[(CO)_5M{=}C(OEt)C{\equiv}CPh]$-$Co_2(CO)_6$, which rearrange to the clusters $MCo_2(CO)_5(\mu\text{-}CO)_2\{\mu_3\text{-}\eta^4\text{-}CC(OEt){=}CPhC(O)\}$ upon thermolysis in boiling hexane [183]. The reaction of $HFe_2Co(CO)_9(\mu_3\text{-}S)$ with $MeCpMo(CO)_3Cl$ in THF leads to the clusters $MeCpMoFeCo(CO)_8(\mu_3\text{-}S)$ and $(MeCp)_2Mo_2Fe(CO)_5(\mu_3\text{-}S)$. Both products were fully characterized in solution and by X-ray crystallography. The mechanism of these electrophilic addition–elimination reactions is discussed [184,185]. Condensation of the tungsten acetylide compounds $Cp^*W(CO)_3(C{\equiv}CR)$ with $Re_2(CO)_6(MeCN)_2$ yields the heterometallic vinylacetylide clusters $Cp^*WRe_2(CO)_9(C{\equiv}CR)$. The acetylide ligand is shown to be coordinated perpendicular to the unique Re–Re bond that is substituted by a bridging CO ligand. The reactivity of these clusters with alcohols and H_2 shows the ease by which the acetylide ligand is converted into μ_3-η^3-allylidene and metallacyclopentadienyl derivatives. A structural discussion on each of the diffraction structures solved is presented [186]. The reversible scission of a coordinated acetylide ligand has been documented. Treatment of $CpWRu_3(CO)_6(C{\equiv}CPh)$ with $Ru_3(CO)_{12}$ at elevated temperature gives the pentanuclear cluster $CpWRu_4(\mu_5\text{-}C)(CO)_{12}(\mu\text{-}CPh)$ and the hexanuclear compound $CpWRu_5(\mu_6\text{-}C)(CO)_{14}(\mu\text{-}CPh)$, as the major and minor products, respectively. The X-ray structures of both carbide clusters have been established (Fig. 19). The reaction of CO with either the WRu_4 or WRu_5 cluster regenerates the initial WRu_3 cluster

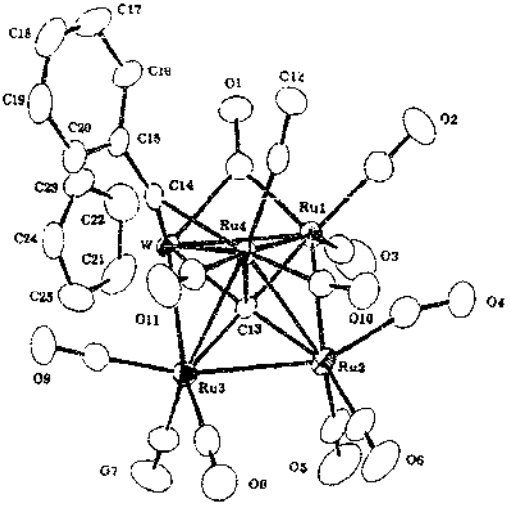

Fig. 19. Structure of $CpWRu_4(\mu_5\text{-}C)(CO)_{12}(\mu\text{-}CPh)$. Reprinted with permission from Journal of the American Chemical Society. Copyright 1994 American Chemical Society.

in near quantitative yield. The acetylide scission scheme and the solution spectroscopic data are discussed [187].

The heterometallic chain compound $MeCpMn(CO)_2(\mu$-dppm)$AuFe\{Si(OMe)_3\}(CO)_3(PPh_3)$ has been isolated from the reaction between $MeCpMn(CO)_2(\mu$-dppm)AuBr and $[Fe\{Si(OMe)_3\}(CO)_3(PPh_3)]^-$. Treatment of $MeCpMn(CO)_2(\eta^1$-dppm) with *trans*-$[Pt\{MeCpW(CO)_3\}_2(NCPh)_2]$ gives the cluster $Pt_2W_2(MeCp)_2(\mu_3$-CO)$(\mu$-CO$)_4[(\mu$-dppm)$Mn(MeCp)(CO)_2]_2$. Cyclic voltammetry data on selected complexes reveal the possibility of electronic communication between different metal centers [188]. Capping-ligand transformations in $Cp'_3MnFe_2(\mu_2$-CO$)_2(\mu_2$-NO$)(\mu_3$-NX) (where Cp′ is Cp, MeCp; X is O, OH, OMe, H) have been studied. The bonding interactions in the conversion of the 48-electron cluster $[Cp_3MnFe_2(\mu_2$-CO$)_2(\mu_2$-NO$)(\mu_3$-NH$)]^+$ to the corresponding 49-electron cluster have been investigated and comparisons made with related trinuclear clusters [189]. The triangular clusters $Re_2(\mu$-PR$_2)(CO)_8[M(CO)_2PPh_3]$ (where M is Rh, Ir; R is Ph, Cy) have been synthesized from the phosphido complex $[Re_2(\mu$-PR$_2)(CO)_8]^-$ and $MCl(CO)(PPh_3)_2$ in the presence of $TlPF_6$ and CO. Use of $[Rh(COD)(PPh_3)_2]^+$ and the anionic phosphido complexes affords the products $ReRh(\mu$-CO$)_2(\mu$-PR$_2)(CO)_3(PPh_3)_2[Re(CO)_4]$, the structure of which contains a Re_2Rh ring and a rhenium–rhodium double bond (Fig. 20) [190].

1,1′-Dialkynylferrocenes react with $Co_2(CO)_8$ to give $[(\eta^5$-$C_5H_4C{\equiv}CR)_2Fe]Co_2(CO)_6$ and $[\{(\eta^5$-$C_5H_4C{\equiv}CR)_2Fe\}Co_2(CO)_6]_2$ [191]. The reactivity of $[\mu$-$\eta^2{:}\eta^2$-$CpFe(CO)_2C{\equiv}CH]Co_2(CO)_6$ under photolysis and thermolysis conditions and in the presence of hydrosilanes has been investigated. The isolated Fe_2Co_3 and $FeCo_3$ clusters have fully characterized in solution by the usual methods [192]. The double butterfly complex $[(OC)_4Fe_2(\mu$-Se$)_2]_2C(Ph)CH$ reacts with

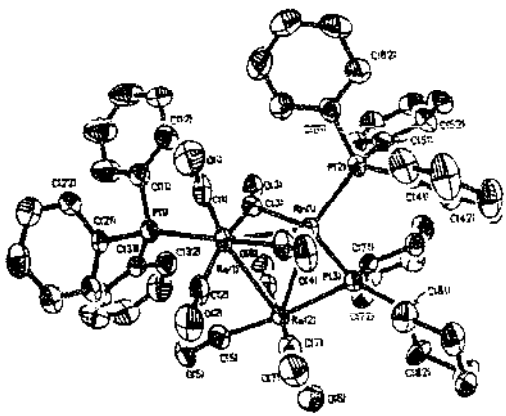

Fig. 20. Structure of $ReRh(\mu$-CO$)_2(\mu$-PR$_2)(CO)_3(PPh_3)_2[Re(CO)_4]$. Reprinted with permission from Inorganic Chemistry. Copyright 1994 American Chemical Society.

Pt(ethylene)(PPh$_3$)$_2$ to yield the diiron complex (OC)$_6$Fe$_2$(μ-SeC(Ph)C(H)Se) and the clusters (OC)$_6$Fe$_2$Pt(PPh$_3$)$_2$(μ-SeC(Ph)C(H)Se) and (OC)$_6$Fe$_2$(μ_3-Se)$_2$Pt(PPh$_3$)$_2$ [193]. The X-ray structure of Fe$_2$(μ-Ag(PPh$_3$))(μ-CO)(CO)$_6$(μ-PBu$^t_2$) and the synthesis of the copper analog have appeared [194]. The reaction between the bimetallic complex (OC)$_3$[(MeO)$_3$Si]Fe(μ-dppm)Hg(C$_6$Cl$_5$) and Pt(PPh$_3$)$_2$(ethylene) gives a 1:1 mixture of the isomeric complexes *trans*- and *cis*-[(OC)$_3$Fe(μ-Si(OMe)$_2$(OMe)](*μ*-dppm)(*μ*-Hg)Pt(C$_6$Cl$_5$)(PPh$_3$)]. The chain core isomerism exhibited by these and other compounds is described [195]. New clusters containing bridging allenyl and allenylcarbonyl ligands have been synthesized. Depending upon the reaction conditions, it is possible to isolate (OC)$_3$Fe(μ_2-CO)RuCp(μ_2-CO)Fe(CO)$_3$(μ_3-η^1-CCH=CHPh), (OC)$_3$FeRuCp(CO)Fe(CO)$_3$(μ_3-η^1:η^1:η^3-CCHCHPh), (OC)$_3$FeFe(CO)$_3$Ru(CO)Cp(μ_3-η^1:η^2:η^2-C(Ph)=C=CH$_2$), and (OC)$_3$FeFe(CO)$_3$Ru(CO)Cp(μ_3-η^1:η^2:η^2-CH=C=CHPh) from the reaction between CpRu(CO)$_2$CH$_2$C≡CPh and Fe$_2$(CO)$_9$. The spectroscopic characterization of these clusters and their reactivity towards added phosphines are described. The X-ray structure of one of the three products determined is shown in Fig. 21 [196].

The X-ray structure of [(Ph$_3$P)$_3$Ir(μ-H)$_3$Ag(μ-H)Ir(PPh$_3$)$_3$]$^+$ reveals the presence of a linear Ir–Ag–Ir array, with the hydride ligands serving to bridge the iridium and silver atoms [197]. The transformation of the carbene cluster Cp*Ir(CpCo)$_2$(μ-CO)$_2$(μ-CH$_2$) into the carbyne cluster Cp*Ir(CpCo)$_2$(μ-CO)(μ_3-CH)(μ-H) is observed in refluxing toluene. The carbyne cluster regenerates the carbene cluster upon exposure to CO. The fluxional behavior involving the exchange of the methylidyne proton and the hydride ligand has been examined and a mechanism involving agostic

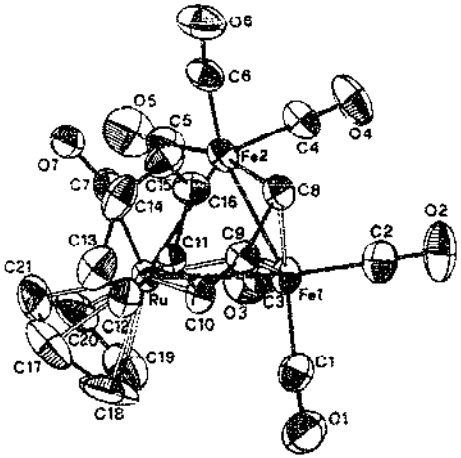

Fig. 21. Structure of (OC)$_3$Fe(μ_2-CO)RuCp(μ_2-CO)Fe(CO)$_3$(μ_3-η^1-CCH=CHPh). Reprinted with permission from Organometallics. Copyright 1994 American Chemical Society.

C–H···M interactions proposed [198]. The synthesis and X-ray structure of the trinuclear cluster $(Ph_3P)_2Ag(\mu\text{-}Cl)_2Co(\mu\text{-}Cl)_2Ag(PPh_3)_2$ have been published [199].

A report dealing with the photoluminescent properties of $Pt_2(AuX)(\mu\text{-dppm})X_2$ and $Pt_2(HgX_2)(\mu\text{-dppm})X_2$ (where X is Cl, Br) has been published. The bonding in these clusters has been studied by carrying out SCF–Xα–SW calculations [200]. XPS data on the clusters $[\{Pt_2(PPh_3)_4(\mu_3\text{-}S)_2Cu\}_2(\mu\text{-dppf})]^{2+}$, $[Pt_2(PPh_3)_4(\mu_3\text{-}S)_2]_2PtCl_2$, and $[\{Pt_2(PPh_3)_4(\mu_3\text{-}S)_2\}_nML]^{n+}$ (where M and L = various metals and ligands) have been collected, and the possibility of distinguishing between chemically inequivalent nuclei is discussed [201]. Neutral $PtAg_2$ clusters possessing unsymmetrical μ_3-σ and μ-η^2, σ alkynyl ligands are reported. Treatment of $[PtAg_2(C_6F_5)_2(C{\equiv}CR)_2]_n$ with PPh_3 leads to the mixed-metal clusters $PtAg_2(C_6F_5)_2,\mu\text{-}\eta^2$, σ-C≡CR)$(\mu_3\text{-}\sigma\text{-}C{\equiv}CR)(PPh_3)_2$ (where R = Ph, Bu^t), of which the phenylacetylene derivative has been characterized by X-ray crystallography [202].

3.2. Tetranuclear clusters

Excess $Cp^*Mo(CO)_3H$ reacts with $Ru_3(CO)_{10}(\mu\text{-}H)(\mu\text{-}PPh_2)$ in refluxing toluene to give the phosphido cluster $Cp^*MoRu_3(CO)_{10}(\mu\text{-}H)_2(\mu\text{-}PPh_2)$ and the phosphinidene cluster $Cp^*MoRu_3(CO)_{10}(\mu_3\text{-}H)(\mu_3\text{-}PPh)$. Both clusters were fully characterized in solution and by X-ray crystallography in the case of the phosphido cluster [203]. The X-ray structure of the butterfly cluster $Cp^*MoRu_3(CO)_{12}H$ has been determined at 110 K, in order to resolve the disorder associated with the μ_4-CO ligand. The X-ray data provide evidence for isomerization of the quadruply bridging CO ligand between the two butterfly isomers. ^{13}C EXSY NMR data and extended Hückel calculations on the barrier to cluster isomerization are discussed [204]. The ketenyl cluster $Os_3(CO)_{10}(\mu\text{-}H)[C(O)CH_2WCp(CO)_3]$ has been synthesized from the reaction between $Os_3(CO)_{10}(MeCN)_2$ and the metallo-aldehyde complex $CpW(CO)_3CH_2CHO$. Pyrolysis of this cluster in the solid state at 185°C leads to $Cp_2W_2Os_3(CO)_{12}(\mu_3\text{-}CMe)$ and $CpWOs_3(CO)_{12}(\mu\text{-}O)(\mu_3\text{-}CMe)$. Both of these pentanuclear clusters arise from the C–O bond scission of the ligated ketene fragment. The latter WOs_3 cluster isomerizes in solution to give the tetrahedral cluster $CpWOs_3(CO)_{12}(\mu_3\text{-}O)(\mu_3\text{-}CMe)$, in which the oxo moiety has migrated from an edge-bridging to face-bridging position. The X-ray structures of all new clusters are presented [205]. Consecutive C–C bond cleavage of an allyl ligand on a WOs_3 cluster is reported. The isomeric allyl clusters $CpWOs_3(CO)_{10}(\mu_3\text{-}\eta^3\text{-}C_3R_2Tol)$ (where R is Tol, Ph), which were prepared from the alkylidyne–alkyne cluster $CpWOs_3(CO)_{10}(\mu_3\text{-}\eta^2\text{-}C_2R_2)(\mu_3\text{-}CTol)$, give the trialkylidyne clusters $CpWOs_3(CO)_9(\mu_3\text{-}CR)_2(\mu_3\text{-}CTol)$ via an alkylidyne–alkyne intermediate. Reaction schemes and two X-ray structures are presented [206]. The antiferromagnetic clusters $Cp_2Cr_2(\mu\text{-}SCMe_3)_2(\mu_2\text{-}S)W_2(\mu_2\text{-}I)_2(CO)_4(NO)_2$ and $Cp_2Cr_2(\mu_3\text{-}S)_2(\mu\text{-}SCMe_3)_2W(SCMe_3)NO$ have been synthesized and characterized in solution [207]. The new clusters $Cp_2Mo_2Fe_2Se_2(CO)_8$ and $Cp_2Mo_2FeSe(CO)_7$, along with the known cluster $Cp_2Mo_2Fe_2Se_3(CO)_6$, are obtained from the thermolysis of $Fe_3(CO)_9Se_2$ and $Cp_2Mo_2(CO)_6$ in benzene. The two new clusters were fully characterized in solution

and by X-ray crystallography [208]. Refluxing $CpWOs_3(CO)_{11}[\mu_3\text{-}\eta^2\text{-}C(O)CH_2Tol]$ in toluene produces the oxo-alkylidyne cluster $CpWOs_3(CO)_9(\mu_3\text{-}O)(\mu_3\text{-}CCH_2Tol)$ as a result of acyl C–O bond cleavage. The reaction of this oxo-capped cluster with CO and H_2 has been examined, and in the case of H_2, the isomeric hydrido-oxo-alkylidene clusters $CpWOs_3(CO)_9(\mu\text{-}H)(\mu\text{-}O)(\mu\text{-}CHCH_2Tol)$ have been isolated. Variable-temperature ^{13}C NMR spectra pertaining to carbonyl scrambling and mechanistic features associated with the cleavage of the acyl C–O bond are discussed [209]. Kinetic studies have been carried out on the sulfido-capped cluster $MeCp_2Mo_2Co_2S_3(CO)_4$. Phosphine and phosphite ligands are shown to react with the parent cluster in a two-step process, where the first steps involves the formation of the adduct cluster $MeCp_2Mo_2Co_2S_3(CO)_4P$, which then loses CO in a subsequent step to give the corresponding substituted cluster. The adduct formed by the addition of PMe_3 has been characterized by X-ray crystallography. The activation parameters are reported and the substitution mechanism discussed [210]. The sequential substitution of CO in $MeCp_2Mo_2Co_2S_3(CO)_4$ by CNR (where R is Me, Bu^t) gives $MeCp_2Mo_2Co_2S_3(CO)_{4-n}(CNR)_n$ (where $n = 1, 2, 3$). The bis-isonitrile derivatives exist as a mixture of cis and trans isomers, as deduced by NMR spectroscopy [211]. The reaction of organic sulfur compounds with $MeCp_2Mo_2Co_2S_3(CO)_4$ is reported to give the cubane cluster $MeCp_2Mo_2Co_2S_4(CO)_2$ in high yield. The products of hydrodesulfurization are discussed relative to the mechanism associated with these reactions [212]. The preparation of the alkylidyne alkyne cluster $CpWOs_3(CO)_{10}(\mu_3\text{-}CMe)(CMeCTol)$ and the dimetalloallyl cluster $CpWOs_3(CO)_9[C(Me)C(Me)C(Tol)]$ from the thermolysis of $Os_3(CO)_{10}(C_2Me_2)$ and $CpW(CO)_2(\equiv CTol)$ is reported. The selective scission of one C–C bond is observed in the dimetalloallyl cluster upon continued thermolysis to give $CpWOs_3(CO)_8(\mu_3\text{-}CTol)(C_2Me_2)$. This last reaction is discussed in the context of alkyne metathesis that proceeds through a dimetalloallyl intermediate. The results of solution characterization (IR and ^{13}C NMR) and two X-ray structures (Fig. 22) are presented [213].

The synthesis of $Re_2Ru_2(\mu\text{-}H)(\mu_3\text{-}S)(\mu\text{-}C_5H_4N)(CO)_{14}$ from $Ru_3(CO)_{12}$ and $Re_2Ru_2(\mu_4\text{-}S)(\mu\text{-}C_5H_4N)(\mu\text{-}pyS)(CO)_{13}$ is described [214]. The sulfido-capped cluster $[Ru_3(CO)_9(\mu_3\text{-}S)]^{2-}$ reacts with $[M(CO)_3(MeCN)_3]^+$ (where M is Mn, Re) to give $HRu_3(CO)_9(\mu_4\text{-}S)M(CO)_3(MeCN)_2$. Use of the cations $[M(CO)_5]^+$ (where M is Mn, Re) gives the clusters $HRu_3(CO)_9(\mu_4\text{-}S)M(CO)_5$. These heterometallic clusters all contain a triangular array of ruthenium atoms with a capping $SM(CO)_3L_2$ moiety (where L is CO, MeCN) [215]. The dynamic NMR behavior of the isomers of $Re_3Pt(\mu\text{-}H)_3(CO)_{14}$ has been explored by NMR spectroscopy [216]. The rhenium carbonyls in $[Pt_3\{Re(CO)_3\}(\mu\text{-dppm})_3]^+$ are ultimately oxidized by added Me_3NO or O_2 to give the oxo cluster $[Pt_3(ReO_3)(\mu\text{-dppm})_3]^+$, the X-ray structure of which has been established (Fig. 23). The bonding in the oxo cluster is discussed in terms of interactions between three filled Pt–Pt bonding orbitals (a_1 and e symmetry) of the $Pt_3(dppm)_3$ fragment and three vacant acceptor orbitals in the ReO_3 fragment [217].

$[H_2Ru_3Rh(CO)_{12}][PPN]$ has been synthesized in high yield from the reaction between $[HRu_3(CO)_{11}][PPN]$ and $Rh_2(CO)_4Cl_2$. The X-ray structure reveals that the cluster is composed of an apical ruthenium atom and a basal Ru_2Rh plane

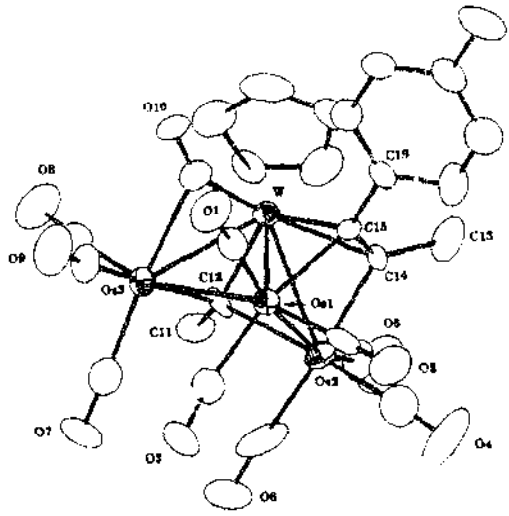

Fig. 22. Structure of $CpWOs_2(CO)_6(\mu_3\text{-}CTol)(C_2Me_2)$. Reprinted with permission from Organometallics. Copyright 1994 American Chemical Society.

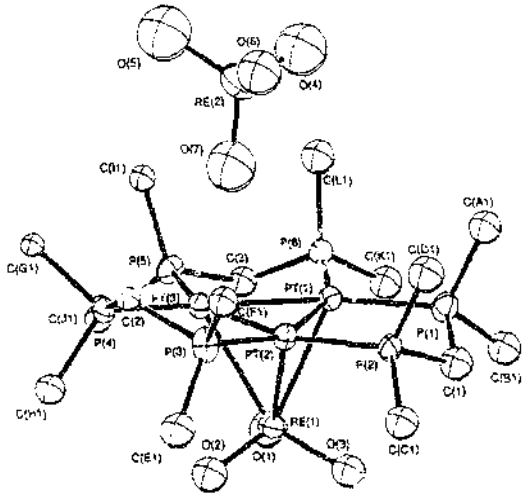

Fig. 23. Structure of $[Pt_3(ReO_3)(\mu\text{-dppm})_3]^+$. Reprinted with permission from Journal of the American Chemical Society. Copyright 1994 American Chemical Society.

[218]. Extended Hückel calculations have been performed on $Fe_3Ru(CO)_{10}(\mu\text{-}CO)(\mu_4\text{-}Se)_2$ and $Fe_4(CO)_{10}(\mu\text{-}CO)(\mu_4\text{-}Se)_2$, and the results discussed with respect to the replacement of one iron atom by a ruthenium atom [219]. Treatment of $[Ru_3(CO)_9BH_4]^-$ and $[Ru_3(CO)_9(B_2H_5)]^-$ with $[Cp^*RhCl_2]_2$ yields the 62-electron butterfly boride-cluster $Ru_3RhCp^*(H)(CO)_9(BH_2)$ and the tetrahedral cluster $Ru_3RhCp^*(H)_2(CO)_{10}$. The iridium dimer $[Cp^*IrCl_2]_2$ reacts with the B_2H_5-substituted ruthenium cluster to give 64-electron cluster $Ru_3IrCp^*(H)(CO)_{10}(BH_2)$ and the tetrahedral cluster $Ru_3RhCp^*(H)_2(CO)_9$. Use of the BH_4-substituted cluster yields only the 64-electron Ru_3Ir cluster [220]. The unsaturated cluster $Os_3H(CO)_8\{Ph_2PCH_2P(Ph)C_6H_4\}$ reacts with $[Au(PPh_3)]^+$ to yield $[Os_3AuH(CO)_8\{Ph_2PCH_2P(Ph)C_6H_4\}]^-$, while reaction with HBF_4 gives the corresponding cationic dihydride cluster $[Os_3H_2(CO)_8\{Ph_2PCH_2P(Ph)C_6H_4\}]^+$. The X-ray structure of the gold derivative accompanies this report [221]. The synthesis and characterization of $MeCpFe_3Co(\mu_4\text{-}S)(CO)_{11}$ have been published. This new cluster, the molecular structure of which has been crystallographically established, was obtained from the reaction between $MeCpFe(CO)_2Cl$ and $HFe_2Co(\mu_3\text{-}S)(CO)_9$ [222]. The results of site-selective substitutions and ligand isomerization in tetrahedral MCo_3 clusters (where M is Fe, Ru) are reported. The X-ray structures of $HRuCo_3(CO)_{10}(PMe_2Ph)_2$ and $HRuCo_3(CO)_9(PMe_2Ph)_3$ are presented [223]. The Fe_3Au butterfly clusters $[Fe_3Au(CO)_{11}(PPh_3)]^-$ and $[\{Fe_3Au(CO)_{11}\}_2(\mu\text{-}L)]^{2-}$ (where L is dppm, dppe) have been prepared and structurally characterized in the case of the PPh_3-substituted cluster (Fig. 24) [224].

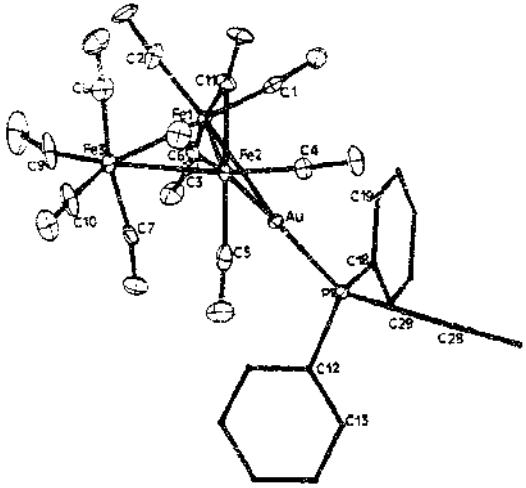

Fig. 24. Structure of $[Fe_3Au(CO)_{11}(PPh_3)]^-$. Reprinted with permission from Organometallics. Copyright 1994 American Chemical Society.

The reaction of diphenylacetylene with $Co_3Rh(CO)_{12}$ under dark and photochemical conditions has been examined, and the X-ray structure of $Co_3Rh(\mu\text{-}CO)_2(CO)_8(\mu_4,\eta^2\text{-}PhC_2Ph)$ presented [225]. The cluster $Ir_3Rh(CO)_8(\eta^4\text{-}COD)_2$ has been synthesized by a redox condensation sequence involving $[Ir(CO)_4]^-$, $[Ir(COD)(THF)_2]^+$, and $[Rh(COD)(THF)_2]^+$. The molecular structure of the Ir_3Rh cluster is based on a tetrahedral core, consisting of an Ir_2Rh basal plane. The COD ligands are readily replaced by added CO to yield $Ir_3Rh(CO)_{12}$ [226].

3.3. *Pentanuclear clusters*

The dangling phosphine moiety in $CpRuCl[(Ph_2P)_2CHCH_2PPh_2]$ replaces up to three CO groups in $Ir_4(CO)_{12}$ to give $Ir_4(CO)_{12-n}[CpRuCl(Ph_2P)_2CHCH_2PPh_2]_n$ (where $n = 1, 2, 3$). These heterometallic clusters were characterized in solution by IR and ^{31}P NMR spectroscopy [227]. Hydride reduction of $Ru_4RhCp^*(CO)_{12}$ using $[Et_4N][BH_4]$ gives the monohydride cluster $[Ru_4RhCp^*(CO)_{11}H]^-$. Treatment of the anionic cluster with iodine leads to $Ru_4RhCp^*(CO)_{11}(H)I$, which has been structurally characterized by X-ray crystallography. The rhodium atom occupies one of the hinge atoms in this wingtip-bridged butterfly cluster. Phosphine substitution chemistry and chloride ion addition reactivity with the parent Ru_4Rh cluster are described [228]. The cluster $Os_3[\mu\text{-}AuOs(CO)_4PPh_3](\mu\text{-}Cl)(CO)_{10}$, prepared from $[Os_4(\mu\text{-}Cl)(CO)_{13}]^-$ and $[Au(PPh_3)]^+$, provides the first example where an $Os(CO)_4$ fragment has inserted into a Au–PPh_3 bond. The X-ray structure of the new cluster is reported [229]. The clusters $[(\mu\text{-}CH_3OCH_2CH{=}C)(\mu\text{-}RS)Fe_2(CO)_6]_2Hg$ (where R is Et, Bu^t) have been isolated from the reaction between $[(\mu\text{-}CO)(\mu\text{-}RS)Fe_2(CO)_6]^-$ and bis(1-alkynyl)mercury compounds. The X-ray structure of the Bu^t derivative is reported [230]. The synthesis and electrochemical examination of Fe_3HgM spiked butterfly clusters have been published. The product anionic clusters are obtained from the reaction between $[Fe_3(CO)_{11}]^{2-}$ and ClHgM [where M is $CpMo(CO)_3$, $CpW(CO)_3$, $CpFe(CO)_2$, $Mn(CO)_5$, $Co(CO)_4$]. Oxidation of these clusters gives the neutral radical clusters, which have been studied by EPR spectroscopy. It is concluded that the unpaired electron is localized in the Fe_3Hg core [231]. The planar triangulated rhomboidal cluster $[Mn_3(CO)_{12}(\mu_3\text{-}H)(\mu\text{-}Hg\{CpMo(CO)_3\})]^-$ has been characterized by X-ray crystallography (Fig. 25). This and related clusters have been synthesized from ClHgM (where M represents various metal compounds) and $[Mn_3(CO)_{12}(\mu\text{-}H)]^-$ in THF solvent. The use of extended Hückel calculations in determining the location of the hydride ligand in the Mn_2Hg rhombus is discussed [232].

3.4. *Hexanuclear clusters*

The reactivity of the unsaturated dihydride complex $Mn_2(\mu\text{-}H)_2(CO)_6[\mu\text{-}(EtO)_2POP(OEt)_2]$ with the acetylide compounds $[M(C{\equiv}CPh)]_n$ (where M is Cu, Ag) has been investigated. The major products isolated have been $Mn_2(\mu\text{-}H)(\mu\text{-}\eta^1{:}\eta^2\text{-}C{\equiv}CPh)(CO)_6[\mu\text{-}(EtO)_2POP(OEt)_2]$ and the hexanuclear clusters $M_2Mn_4(\mu\text{-}H)_6(CO)_{12}[\mu\text{-}(EtO)_2POP(OEt)_2]_2$, which in the case of the silver deriva-

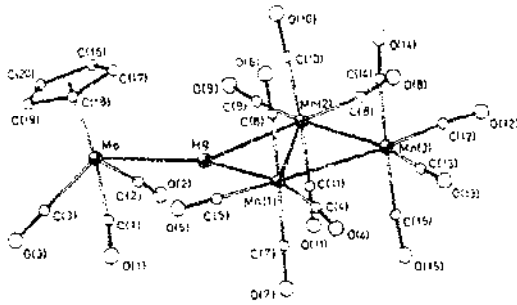

Fig. 25. Structure of $[Mn_3(CO)_{13}(\mu_3\text{-}H)(\mu\text{-}Hg)CpMo(CO)_2]$. Reprinted with permission from Organometallics. Copyright 1994 American Chemical Society.

tive has been characterized by X-ray crystallography. Use of $[Au(C{\equiv}CPh)]_n$ affords the cluster $AuMn_4(\mu\text{-}H)_5(CO)_{12}[\mu\text{-}(EtO)_2POP(OEt)_2]$. The fluxional properties of these clusters and the adopted polyhedral geometries are fully discussed [233]. The boride clusters $[Ru_4Rh_2(CO)_{16}B]^-$ and $[Ru_6Rh_3(CO)_{23}B_2]^-$ have been prepared and characterized in the solid state by X-ray crystallography. The former cluster possesses two trans rhodium atoms, along with an interstitial boride atom [234]. The cluster $Ru_5RhCp^*(C)(CO)_{14}$ undergoes fragmentation under high CO pressure to give $Ru_3(CO)_{12}$, $Ru_5C(CO)_{15}$, and the new cluster $Ru_4RhCp^*(C)(CO)_{12}$, the molecular structure of which has been solved. The Ru_4Rh polyhedron is based on a square-based pyramid. The reactivity of the starting Ru_5Rh cluster with methoxide has also been examined [235]. $Ru_4Pt_2(CO)_{14}$ reacts with H_2 to give the new cluster $Ru_6Pt_3(CO)_{21}(\mu\text{-}H)_3(\mu_3\text{-}H)$ in 83% yield. The molecular structure consists of three triangular arrays of nine metal atoms, giving rise to the observed face-shared bioctahedron. The outer layers are composed of ruthenium triangles, with the three platinum atoms forming the central layer. Diphenylacetylene reacts with this Ru_6Pt_3 cluster to afford the alkyne cluster $Ru_6Pt_3(CO)_{20}(\mu_3\text{-}PhC_2Ph)(\mu_3\text{-}H)(\mu\text{-}H)$. The X-ray structure of this cluster (Fig. 26) confirms the coordination mode adopted by the alkyne ligand. The transformation of the alkyne ligand in this cluster to an edge bridging σ-π coordinated diphenylvinyl ligand has been documented [236].

A report describing the surface-mediated synthesis of $[Rh_5Pt(CO)_{15}]^-$ on MgO has appeared [237].

3.5. *Higher nuclearity clusters*

The prismatic structure of $Pt_6Hg(2,6\text{-}Me_2C_6H_3NC)_{12}$ has been confirmed by X-ray crystallography. The six platinum atoms define the trigonal prism core, with the mercury atom situated in a pseudocenter location of the prismatic core. The bonding in this cluster was also explored by carrying out XPS measurements and extended Hückel calculations [238]. The synthesis of $[Fe_3(CO)_9Se]^{2-}$ and its reaction with $M(OAc)_2$ (where M is Hg, Cd) to give the clusters $[\{Fe_3(CO)_9Se\}_2M]^{2-}$ are reported.

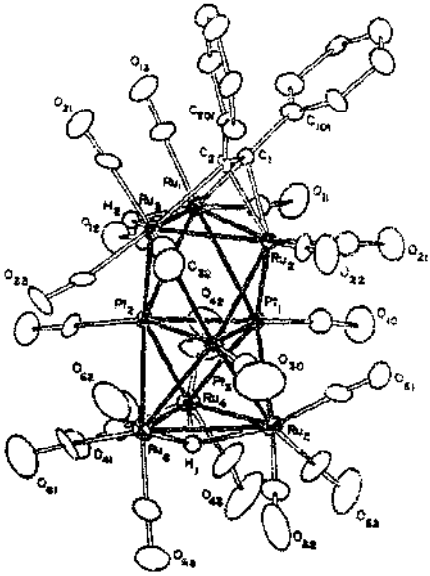

Fig. 26. Structure of $Ru_6P_2(CO)_{20}(\mu_3\text{-}PhC_2Ph)(\mu_3\text{-}H)(\mu\text{-}H)$. Reprinted with permission from Organometallics. Copyright 1994 American Chemical Society.

The potential for these linked clusters to serve as building blocks for other higher-nuclearity clusters is discussed [239]. Deprotonation of $Fe_3(CO)_9(\mu_3\text{-}PMe)(\mu_3\text{-}PH_2)$, followed by phosphine functionalization, has been used as a route for the synthesis of extended cluster chains. Trapping the intermediate anion $[Fe_3(CO)_9(\mu_3\text{-}PMe)(\mu_3\text{-}P)]^-$ with ClAu(THT) gives the new cluster $[\{Fe_3(CO)_9(\mu_3\text{-}PMe)(\mu_3\text{-}P)\}_2Au]^-$, the molecular structure of which has been crystallographically determined [240]. Spectroscopic data are presented for the formation of $Rh_6N(CO)_{15}[Au(PPh_3)]$, which was prepared from $[Rh_6N(CO)_{15}]^-$ and Au(PPh$_3$)Cl. Au(PPh$_3$)Cl reacts with $[Rh_6C(CO)_{15}]^{2-}$ at −80°C to give $[Rh_6C(CO)_{15}\{Au(PPh_3)\}]^-$; NMR studies reveal that the Au(PPh$_3$) moiety rapidly migrates about the octahedral core at −80°C. Warming to room temperature leads to CO loss and formation of $[Rh_6C(CO)_{12}\{Au(PPh_3)\}_3]^-$, which has been characterized in solution by multinuclear NMR measurements [241]. The carbide cluster $[Ru_5C(CO)_{14}]^{2-}$ reacts with excess $[Rh(COD)_2]^+$ to furnish the monoanion $[Ru_5RhC(CO)_{14}(COD)]^-$, which may be protonated by $HBF_4{\cdot}OEt_2$ to give $Ru_5RhH(C)(CO)_{14}(COD)$. The reactivity of the anionic Ru_5Rh cluster with the gold reagents Au(PPh$_3$)Cl and Au(PEt$_3$)Cl has also been studied. The X-ray structure of $Ru_5RhC(CO)_{14}(COD)\{\mu_3\text{-}Au(PPh_3)\}$ accompanies this report [242]. The synthesis and X-ray structure of $[Os_6Pd(CO)_{18}(bpy)$ have been published. This new cluster is

obtained from the reaction between $Os_3(CO)_{10}(MeCN)_2$ and $Pd(bpy)(CO_2Me)_2$. The X-ray structure of the Os_6Pd cluster is based on a monocapped octahedron with the palladium atom functioning as one of the octahedral vertices [243]. $[Os_8(CO)_{22}][PPN]_2$ has been allowed to react with $Au_2Cl_2(P\ P)$ (where P P is dppm, dppe, dppb) in the presence of $TlPF_6$ to yield the mixed-metal clusters $Os_8(CO)_{22}[Au_2(P\ P)]$ in near quantitative yield. In the case of the dppb derivative, X-ray diffraction analysis reveals that the cluster is composed of a bicapped octahedron of osmium atoms, with one of the gold atoms capping the osmium octahedron, and the other gold atom bridging an edge of the osmium core [244]. The preparation, molecular structure (Fig. 27), and polyhedral skeletal isomerization in $[Re_7IrC(CO)_{25}]^{2-}$ have been reported [245].

D_2/H_2O isotope exchange using the platinum–gold cluster $[Pt(AuPPh_3)_8]^{2+}$ has been achieved. NMR data on the cluster species present in solution and a working catalytic mechanism are discussed [246]. Metallic mercury adds to $[Pt(PPh_3)(AuPPh_3)_6]^{2+}$ to produce $[Pt(PPh_3)(AuPPh_3)_6(HgNO_3)]^+$, the molecular structure of which has been crystallographically determined. The displacement of metallic mercury from this cluster and the reactivity toward $[Co(CO)_4]^-$ are described [247]. The clusters $[Ag_4\{\mu_2\text{-}Fe(CO)_4\}_4]^{4-}$ and $[Ag_5\{\mu_2\text{-}Fe(CO)_4\}_2\{\mu_3\text{-}Fe(CO)_4\}_2]^{3-}$ have been prepared and the electron counts rationalized by extended Hückel calculations. The X-ray structure of the former cluster is shown in Fig. 28 [248].

The reaction of $[CuCl_2(PPh_3)]^-$ with $[Fe_2(CO)_6(\mu_2\text{-}S)_2]^{2-}$ in MeCN/MeOH leads to the iron–copper–sulfur cluster $[Fe_6Cu_6(\mu_4\text{-}S)_6(CO)_{18}(PPh_3)_2]^-$. The X-ray structure of the new cluster has been solved [249]. Treatment of $[Ru_3H(CO)_{11}]^-$ with $Pd(PhCN)_2Cl_2$ affords the cluster $[Ru_6Pd_6(CO)_{24}]^{2-}$, which is shown to possess a trigonally distorted octahedron of palladium atoms that is capped by ruthenium

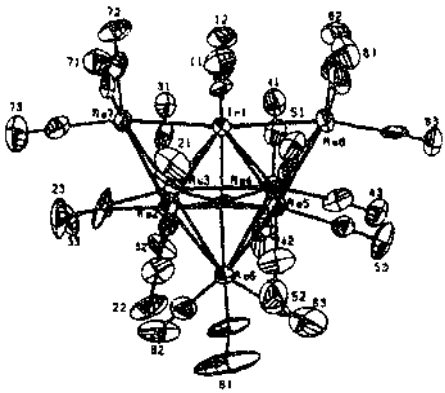

Fig. 27. Structure of $[Re_7IrC(CO)_{25}]^{2-}$. Reprinted with permission from Journal of the American Chemical Society. Copyright 1994 American Chemical Society.

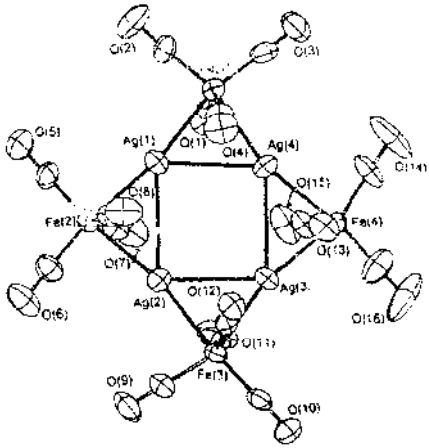

Fig. 28. Structure of $[Ag_4\{\mu_3\text{-}Fe(CO)_4\}_4]^{4-}$. Reprinted with permission from Inorganic Chemistry. Copyright 1994 American Chemical Society.

atoms by X-ray diffraction analysis. The ^{13}C NMR data and electrochemical behavior of this cluster are presented [250]. The carbide cluster $[Rh_{12}C_2(CO)_{23}(AuPPh_3)]^-$ has been isolated from the reaction between $Au(PPh_3)Cl$ and $[Rh_{12}C_2(CO)_{24}]^{2-}$. The solution and solid-state structures of this cluster have been determined and discussed relative to how the CO ligands are distributed about the cluster polyhedron [251].

4. Abbreviations

acac	acetylacetonate
ampy	2-amino-6-methylpyridinate
bpm	2,2′-bipyrimidine
bpy	2,2′-bipyridine
COD	1,5-cyclooctadiene
Cp	cyclopentadienyl
Cp*	pentamethylcyclopentadienyl
Cy	cyclohexyl
dmpm	bis(dimethylphosphino)methane
dppb	1,4-bis(diphenylphosphino)butane
dppe	1,2-bis(diphenylphosphino)ethane
dppf	1,1′-bis(diphenylphosphino)ferrocene
dppm	bis(diphenylphosphino)methane

dppp	1,3-bis(diphenylphosphino)propane
Fc	ferrocenyl
mbim	2-mercaptobenzimidazolate
Mes	mesityl
mnt	1,2-dicyanoethane-1,2-dithiolate
PPN	bis(triphenylphosphine)iminium
py	pyridine
pyS	pyridine-2-thionato
THT	tetrahydrothiophene
TMS	trimethylsilyl
Tol	tolyl
XPS	X-ray photoelectron spectroscopy

References

[1] J.A. Shipley, Diss. Abstr. B, 54 (1994) 5658, DANN83762.
[2] A.K.-Y. Ma, Diss. Abstr. B, 54 (1994) 5655, DANN83617.
[3] G. Kong, Diss. Abstr. B, 54 (1994) 4149, DA9404097.
[4] A.J. Whoolery, Diss. Abstr. B, 54 (1994) 4666, DA9330266.
[5] W. Li, Diss. Abstr. B, 54 (1994) 5655, DA9412496.
[6] R.J. Donovan, Diss. Abstr. B, 55 (1994) 411, DA9417810.
[7] R.A. Heintz, Diss. Abstr. B, 54 (1994) 6194, DA9416693.
[8] K.J. Deck, Diss. Abstr. B, 55 (1994) 2209, DA9428003.
[9] Y. Zheng, Diss. Abstr. B, 55 (1994) 895, DANN86394.
[10] A.S.L. Ma, Diss. Abstr. B, 55 (1994) 892, DA9410615.
[11] D. Solooki, Diss. Abstr. B, 55 (1994) 1431, DA9425858.
[12] F.A. Kvietok, Diss. Abstr. B, 55 (1994) 1430, DA9423515.
[13] T.C. Zheng, Diss. Abstr. B, 55 (1994) 421, DANN85444.
[14] H. Zhang, Diss. Abstr. B, 55 (1994) 420, DANN85413.
[15] H.A. Mirza, Diss. Abstr. B, 54 (1994) 4151, DANN81271.
[16] D.A. Morgenstern, Diss. Abstr. B, 54 (1994) 3616, DA9334400.
[17] D.L. Sunick, Diss. Abstr. B, 54 (1994) 6199, DA9415394.
[18] Y. Koide, Diss. Abstr. B, 55 (1994) 414, DA9415342.
[19] M.T. Bautista, Diss. Abstr. B, 55 (1994) 2207, DA9429385.
[20] R. Andrés, M.V. Galakhov, A. Martín, M. Mena and C. Santamaría, Organometallics, 13 (1994) 2159.
[21] A. Herzog, F.-Q. Liu, H.W. Roesky, A. Demsar, K. Keller, M. Noltemeyer and F. Pauer, Organometallics, 13 (1994) 1251.
[22] B. Zhuang, P. Yu, L. Huang, L. He and J. Lu, Polyhedron, 13 (1994) 125.
[23] L.Y. Goh and W. Chen, J. Chem. Soc. Dalton Trans., (1994) 2697.
[24] R.A. Heintz, R.L. Ostrander, A.L. Rheingold and K.H. Theopold, J. Am. Chem. Soc., 116 (1994) 11387.
[25] F. Bottomley, J. Chen, J.F. Preston and R.C. Thompson, J. Am. Chem. Soc., 116 (1994) 7989.
[26] J.T. Lin, S.Y. Wang, A.C. Yeh, T.Y.R. Tsai, S.-M. Peng, G.H. Lee and Y.S. Wen, Inorg. Chem., 33 (1994) 1948.
[27] R. Alberto, A. Egli, U. Abram, K. Hegetschweiler, V. Gramlich and P.A. Schubiger, J. Chem. Soc. Dalton Trans., (1994) 2815.
[28] P.D. Lane and J.R. Shapley, J. Mol. Catal., 86 (1994) 121.
[29] R.D. Adams and S.B. Falloon, J. Am. Chem. Soc., 116 (1994) 10540.

[30] C.S. Yang and C.P. Cheng, J. Chem. Soc. Dalton Trans., (1994) 2011.
[31] G. Hsu, S.R. Wilson and J.R. Shapley, Organometallics, 13 (1994) 4159.
[32] B.C. Gates, J. Mol. Catal., 86 (1994) 95.
[33] G. Jenner, J. Organomet. Chem., 469 (1994) 99.
[34] F.-W. Grevels, W.E. Klotzbücher, J. Schrickel and K. Schaffner, J. Am. Chem. Soc., 116 (1994) 6229.
[35] A. Bassoli, S. Cenini, F. Farina, M. Orlandi and B. Rindone, J. Mol. Catal., 89 (1994) 121.
[36] S.L. Scott and J.-M. Basset, J. Mol. Catal., 86 (1994) 5.
[37] L. Alvila, J. Pursiainen, J. Kivialho, T.A. Pakkanen and O. Krause, J. Mol. Catal., 91 (1994) 335.
[38] D. Braga, L. Farrugia, F. Grepioni and B.F.G. Johnson, J. Organomet. Chem., 464 (1994) C39.
[39] D. Braga, F. Grepioni, L.J. Farrugia and B.F.G. Johnson, J. Chem. Soc. Dalton Trans., (1994) 2911.
[40] M.R. Burke, T. Funk, J. Takats and V.W. Day, Organometallics, 13 (1994) 2109.
[41] Y. Kabe, T. Yamamoto and W. Ando, Organometallics, 13 (1994) 4606.
[42] J.-F. Riehl, N. Koga and K. Morokuma, Organometallics, 13 (1994) 4765.
[43] J.-F. Riehl, N. Koga and K. Morokuma, J. Am. Chem. Soc., 116 (1994) 5414.
[44] H. Suzuki, Y. Takaya, T. Takemori and M. Tanaka, J. Am. Chem. Soc., 116 (1994) 10779.
[45] L.V. Rybin, S.V. Osintseva, P.V. Petrovskii, M.I. Rybinskaya, F.M. Dolgushin, A.I. Yanovsky and Y.T. Struchkov, J. Organomet. Chem., 479 (1994) C25.
[46] T.P. Jeynes, M.P. Cifuentes, M.G. Humphrey, G.A. Koutsantonis and C.L. Raston, J. Organomet. Chem., 476 (1994) 133.
[47] M.R. Churchill, C.H. Lake, W. Paw and J.B. Keister, Organometallics, 13 (1994) 8.
[48] D.S. Bohle, K.T. Carron, A.N. Christensen, P.A. Goodson and A.K. Powell, Organometallics, 13 (1994) 1355.
[49] D.J. Darensbourg, B. Fontal, S.S. Chojnacki, K.K. Klausmeyer and J.H. Reibenspies, Inorg. Chem., 33 (1994) 3526.
[50] M. Koike, D.G. Van der Velde and J.R. Shapley, Organometallics, 13 (1994) 1404.
[51] S. Aime, W. Dastrú, R. Gobetto and A.J. Arce, Organometallics, 13 (1994) 3737.
[52] J.W.M. van Outersterp, F. Hartl and D.J. Stufkens, Inorg. Chem., 33 (1994) 2711.
[53] M. Koike and J.R. Shapley, J. Organomet. Chem., 470 (1994) 199.
[54] A.A. Koridze, N.M. Astakhova, P.V. Petrovskii, F.M. Dolgushin, A.I. Yanovsky and Y.T. Struchkov, J. Organomet. Chem., 481 (1994) 247.
[55] H.G. Ang, B. Chang, W.L. Kwik and E.S.H. Sim, J. Organomet. Chem., 474 (1994) 153.
[56] H.G. Ang, W.L. Kwik and K.K. Ong, J. Organomet. Chem., 474 (1994) 149.
[57] W.-Y. Yeh, S.-B. Chen, S.-M. Peng and G.-H. Lee, J. Organomet. Chem., 481 (1994) 183.
[58] O. bin Shawkataly, S.-G. Teoh and H.-K. Fun, J. Organomet. Chem., 464 (1994) C29.
[59] K.-L. Lu, H.-J. Chen, P.-Y. Lu, S.-Y. Li, F.-E. Hong, S.-M. Peng and G.-H. Lee, Organometallics, 13 (1994) 585.
[60] S.E. Kabir, A. Miah, K. Uddin and A.J. Deeming, J. Organomet. Chem., 476 (1994) 121.
[61] M.D. Soucek, C.C. Clubb, E.P. Kyba, D.S. Price, V.G. Schenler, H.O. Aldaz-Palacios and R.E. Davis, Organometallics, 13 (1994) 1120.
[62] T.C. Zheng, W.R. Cullen and S.J. Rettig, Organometallics, 13 (1994) 3594.
[63] A.J. Deeming, R. Vaish, A.J. Arce and Y. De Sanctis, Polyhedron, 13 (1994) 3285.
[64] S. Jeannin, Y. Jeannin, F. Robert and C. Rosenberger, Inorg. Chem., 33 (1994) 243.
[65] S. Jeannin, Y. Jeannin, F. Robert and C. Rosenberger, J. Organomet. Chem., 480 (1994) 111.
[66] R.E. Bachman and K.H. Whitmire, Inorg. Chem., 33 (1994) 2527.
[67] E.W. Amscough, A.M. Brodie, S.L. Ingham, T.G. Kotch, A.J. Lees, J. Lewis and J.M. Waters, J. Chem. Soc. Dalton Trans., (1994) 1.
[68] Z.-G. Fang, P.M.N. Low, S.-C. Ng and T.S.A. Hor, J. Organomet. Chem., 483 (1994) 17.
[69] T. Mitsui, S. Inomata and H. Ogino, Inorg. Chem., 33 (1994) 4934.
[70] H. Hashimoto, H. Tobita and H. Ogino, Organometallics, 13 (1994) 1055.
[71] R. Rumin, F.R.-L. Guen, J. Talarmin and F.Y. Petillon, Organometallics, 13 (1994) 1155.
[72] G.B. Karet, D.M. Norton, C.L. Stern and D.F. Shriver, Inorg. Chem., 33 (1994) 5750.
[73] S. Aime, W. Dastrú, R. Gobetto and A.J. Arce, Organometallics, 13 (1994) 4232.
[74] S. Chan, W.-Y. Wong and W.-T. Wong, J. Organomet. Chem., 474 (1994) C30.

[75] K.-L. Lu, M.-L. Chung, P.-Y. Lu, H.-M. Gau, F.-E. Hong and Y.-S. Wen, Organometallics, 13 (1994) 3177.
[76] K.-L. Lu, L.-K. Liu, C.-J. Su, H.-M. Gau, Y. Wang and G.-H. Lee, J. Organomet. Chem., 482 (1994) 67.
[77] A.J. Arce, A.J. Deeming, Y. De Sanctis, A.M. Garcia, J. Manzur and E. Spodine, Organometallics, 13 (1994) 3381.
[78] L. Girard, A. Decken, A. Bleeking and M.J. McGlinchey, J. Am. Chem. Soc., 116 (1994) 6427.
[79] M.P. Cifuentes, M.G. Humphrey, B.W. Skelton and A.H. White, J. Organomet. Chem., 466 (1994) 211.
[80] K.J. Adams, J.J. Barker, J.P.H. Charmant, C. Ganter, G. Klatt, S.A.R. Knox, A.G. Orpen and S. Ruile, J. Chem. Soc. Dalton Trans., (1994) 477.
[81] S.E. Kabir, E. Rosenberg, M. Day and K.I. Hardcastle, Organometallics, 13 (1994) 4437.
[82] L.E. Crascall, B.H.S. Thimmappa, A.L. Rheingold, R. Ostrander and T.P. Fehlner, Organometallics, 13 (1994) 2153.
[83] J.A. Cabeza, R.J. Franco and V. Riera, Inorg. Chem., 33 (1994) 5952.
[84] W. Trakarnpruk, A.M. Arif and R.D. Ernst, Organometallics, 13 (1994) 2423.
[85] B.F.G. Johnson, J. Organomet. Chem. 475 (1994) 31.
[86] P.J. Dyson, B.F.G. Johnson, C.M. Martin, A.J. Blake, D. Braga, F. Grepioni and E. Parisini, Organometallics, 13 (1994) 2113.
[87] K.-L. Lu, S. Kumaresan, Y.-S. Wen and J.R. Hwu, Organometallics, 13 (1994) 3170.
[88] J.A. Cabeza, R.J. Franco, A. Llamazares, V. Riera, E. Pérez-Carreño and J.F. Van der Maelen, Organometallics, 13 (1994) 55.
[89] J.A. Cabeza, J. Fernández-Colinas, S. García-Granda, A. Llamazares, F. López-Ortiz, V. Riera and J.F. Van der Maelen, Organometallics, 13 (1994) 426.
[90] S. Alvarez, P. Briard, J.A. Cabeza, I. del Rio, J.M. Fernández-Colinas, F. Mulla, L. Ouahab and V. Riera, Organometallics, 13 (1994) 4360.
[91] J.A. Cabeza, A. Llamazares, V. Riera, P. Briard and L. Ouahab, J. Organomet. Chem., 480 (1994) 205.
[92] J.A. Cabeza, J.M. Fernández-Colinas, A. Llamazares, V. Riera, S. García-Granda and J.F. Van der Maelen, Organometallics, 13 (1994) 4352.
[93] R.D. Adams, X. Qu and W. Wu, Organometallics, 13 (1994) 1272.
[94] R.D. Adams, L. Chen and X. Qu, Organometallics, 13 (1994) 1092.
[95] J.F. Corrigan, M. Dmardo, S. Doherty, G. Hogarth, Y. Sun, N.J. Taylor and A.J. Carty, Organometallics, 13 (1994) 3572.
[96] J.F. Corrigan, S. Doherty, N.J. Taylor and A.J. Carty, J. Am. Chem. Soc., 116 (1994) 9799.
[97] J.F. Corrigan, N.J. Taylor and A.J. Carty, Organometallics, 13 (1994) 3778.
[98] M.I. Bruce, J.R. Hinchliffe, R. Surynt, B.W. Skelton and A.H. White, J. Organomet. Chem., 469 (1994) 89.
[99] A. Selvini, P. Frediani, D. Rovai, M. Bianchi and F. Piacenti, J. Mol. Catal., 89 (1994) 77.
[100] P. Zanello, F. Laschi, A. Cinquantini, R.D. Pergola, L. Garlaschelli, M. Cucco, F. Demartin and T.R. Spalding, Inorg. Chim. Acta, 226 (1994) 1.
[101] S. Schrölkamp, W. Sperber, D. Lentz and W.P. Fehlhammer, Chem. Ber., 127 (1994) 621.
[102] B.F.G. Johnson, A.J. Blake, C.M. Martin, D. Braga, E. Parisini and H. Chen, J. Chem. Soc. Dalton Trans., (1994) 2167.
[103] G. Meister, G. Rheinwald, H. Stoeckli-Evans and G. Süss-Fink, J. Chem. Soc. Dalton Trans., (1994) 3215.
[104] J.R. Galsworthy, C.E. Housecroft, J.S. Humphrey, X. Song, A.J. Edwards and A.L. Rheingold, J. Chem. Soc. Dalton Trans., (1994) 3273.
[105] S. Inomata, K. Hiyama, H. Tobita and H. Ogino, Inorg. Chem., 33 (1994) 5337.
[106] D. Roberto, E. Cariati, R. Psaro and R. Ugo, Organometallics, 13 (1994) 734.
[107] S. Aime, R. Gobetto, A. Orlandi, C.J. Groombridge, G.E. Hawkes, M.D. Mantle and K.D. Sales, Organometallics, 13 (1994) 2375.
[108] W. Wang, H.B. Davis, F.W.B. Einstein and R.K. Pomeroy, Organometallics, 13 (1994) 5113.
[109] D.H. Farrar, A.J. Pöe and Y. Zheng, J. Am. Chem. Soc., 116 (1994) 6252.

[110] C.J. Adams, M.I. Bruce, M. Schulz, B.W. Skelton and A.H. White, J. Organomet. Chem., 472 (1994) 285.
[111] P.J. Dyson, B.F.G. Johnson and D. Braga, Inorg. Chim. Acta, 222 (1994) 299.
[112] W. van den Berg, C.E. Boot, J.G.M. van der Linden, W.P. Bosman, J.M.M. Smits, P.T. Beurskens and J. Heck, Inorg. Chim. Acta, 216 (1994) 1.
[113] S. Inomata, K. Hitomi, H. Tobita and H. Ogino, Inorg. Chim. Acta, 225 (1994) 229.
[114] D. Braga, P. Sabatino, P.J. Dyson, A.J. Blake and B.F.G. Johnson, J. Chem. Soc. Dalton Trans., (1994) 393.
[115] D. Braga, P.J. Dyson, F. Grepioni, B.F.G. Johnson and M.J. Calhorda, Inorg. Chem., 33 (1994) 3218.
[116] W. Wang, F.W.B. Einstein and R.K. Pomeroy, Organometallics, 13 (1994) 1114.
[117] R.D. Adams, S.B. Falloon and K.T. McBride, Organometallics, 13 (1994) 4870.
[118] M.P. Cifuentes, T.P. Jeynes, M.G. Humphrey, B.W. Skelton and A.H. White, J. Chem. Soc. Dalton Trans., (1994) 925.
[119] J. Lewis, C.-K. Li, C.A. Morewood, M.C.R. de Arellano, P.R. Raithby and W.-T. Wong, J. Chem. Soc. Dalton Trans., (1994) 2159.
[120] D.M. Norton, C.L. Stern and D.F. Shriver, Inorg. Chem., 33 (1994) 2701.
[121] T. Chihara and H. Yamazaki, J. Organomet. Chem., 473 (1994) 273.
[122] A.J. Blake, P.J. Dyson, R.C. Gash, B.F.G. Johnson and P. Trickey, J. Chem. Soc. Dalton Trans., (1994) 1105.
[123] D. Braga, F. Grepioni, C.M. Martin, E. Parisini, P.J. Dyson and B.F.G. Johnson, Organometallics, 13 (1994) 2170.
[124] M. Shieh and M.-H. Shieh, Organometallics, 13 (1994) 920.
[125] L.H. Gade, B.F.G. Johnson, J. Lewis, M. McPartlin, H.R. Powell, P.R. Raithby and W.-T. Wong, J. Chem. Soc. Dalton Trans., (1994) 521.
[126] R.B. King, J. Organomet. Chem., 478 (1994) 13.
[127] E. Charalambous, L. Heuer, B.F.G. Johnson, J. Lewis, W.-S. Li, M. McPartlin and A.D. Massey, J. Organomet. Chem., 468 (1994) C9.
[128] T.P. Fehlner, J. Organomet. Chem., 478 (1994) 49.
[129] A. Bandyopadhyay, M. Shang, C.S. Jun and T.P. Fehlner, Inorg. Chem., 33 (1994) 3677.
[130] A.R. Manning, L. O'Dwyer, P.A. McArdle and D. Cunningham, J. Organomet. Chem., 474 (1994) 173.
[131] M. Breza, Polyhedron, 13 (1994) 103.
[132] B.-S. Kang, Y.-J. Xu, X.-L. Xie, C.-N. Chen, Q.-T. Liu, H.-Q. Liu and J.-X. Lu, Inorg. Chem., 33 (1994) 3770.
[133] M.-J. Don, H.-Y. Chien and M.G. Richmond, J. Mol. Catal., 88 (1994) 133.
[134] K. Yang, H.-Y. Chien and M.G. Richmond, J. Mol. Catal., 88 (1994) 159.
[135] J. Borgdorff, N.W. Duffy, B.H. Robinson and J. Simpson, Inorg. Chim. Acta, 224 (1994) 73.
[136] D.L. Vollmer, M.L. Gross, R.J. Waugh, M.I. Bruce and J.H. Bowie, Organometallics, 13 (1994) 3564.
[137] N.W. Duffy, B.H. Robinson, K. Robinson and J. Simpson, J. Chem. Soc. Dalton Trans., (1994) 2821.
[138] M.P. Robben, W.E. Geiger and A.L. Rheingold, Inorg. Chem., 33 (1994) 5615.
[139] P. Quéneau'h, R. Rumin and F.Y. Pétillon, J. Organomet. Chem., 479 (1994) 93.
[140] M.C. Comstock, S.R. Wilson and J.R. Shapley, Organometallics, 13 (1994) 3805.
[141] F. Asseid, J. Browning, K.R. Dixon and N.J. Meanwell, Organometallics, 13 (1994) 760.
[142] C.P. Casey, R.A. Widenhoefer, S.L. Hallenbeck, R.K. Hayashi, D.R. Powell and G.W. Smith, Organometallics, 13 (1994) 1521.
[143] C.P. Casey, R.A. Widenhoefer, S.L. Hallenbeck and R.K. Hayashi, Inorg. Chem., 33 (1994) 2639.
[144] C.P. Casey, R.A. Widenhoefer, S.L. Hallenbeck, R.K. Hayashi and J.A. Gaveny, Jr., Organometallics, 13 (1994) 4720.
[145] B.F.G. Johnson, Y.V. Roberts, E. Parisini and R.E. Benfield, J. Organomet. Chem., 478 (1994) 21.
[146] R.D. Perola, F. Cea, L. Garlaschelli, V. Maseiocchi and M. Sansoni, J. Chem. Soc. Dalton Trans., (1994) 1501.
[147] Y. Nishihara, K.J. Deck, M. Shang, T.P. Fehlner, B.S. Haggerty and A.L. Rheingold, Organometallics, 13 (1994) 4510.

[148] S. Schulz, M. Andruh, T. Pape, T. Heinze, H.W. Roesky, L. Häming, A. Kuhn and R. Herbst-Irmer, Organometallics, 13 (1994) 4004.
[149] K.R. Dunbar, J.H. Matonic and V.P. Saharan, Inorg. Chem., 33 (1994) 25.
[150] G. Fachinetti, G. Fochi and T. Funaioli, Inorg. Chem., 33 (1994) 1719.
[151] D.A. Dobbs and R.G. Bergman, Inorg. Chem., 33 (1994) 5329.
[152] T. Nishioka, V.Y. Kukushkin, K. Isobe and A. Vázquez de Miguel, Inorg. Chem., 33 (1994) 2501.
[153] S. Kawi, Z. Xu and B.C. Gates, Inorg. Chem., 33 (1994) 503.
[154] T. Blum, M.P. Brown, B.T. Heaton, A.S. Hor, J.A. Iggo, J.S.Z. Sabounchei and A.K. Smith, J. Chem. Soc. Dalton Trans., (1994) 513.
[155] G. Ciani, D.M. Proserpio, A. Sironi, S. Martinengo and A. Funaioli, J. Chem. Soc. Dalton Trans., (1994) 471.
[156] S.P. Tunik, A.V. Vlasov, K.V. Kogdov, G.L. Starova, A.B. Nikol'skii, O.S. Manole and Y.T. Struchkov, J. Organomet. Chem., 479 (1994) 59.
[157] B.W. Clare, M.C. Favas, D.L. Kepert, A.S. May and N.R. Taylor, J. Organomet. Chem., 478 (1994) 111.
[158] G. Sánchez, F. Ruiz, M.D. Santana, G. García, G. López, J.A. Hermoso and M. Martínez-Ripoll, J. Chem. Soc. Dalton Trans., (1994) 19.
[159] M. Rushidi, J.J. Vittal and R.J. Puddephatt, J. Chem. Soc. Dalton Trans., (1994) 1283.
[160] T. Tanase, H. Ukaji, Y. Kudo, M. Ohno, K. Kobayashi and Y. Yamamoto, Organometallics, 13 (1994) 1374.
[161] R. Provencher, K.T. Ayc, M. Drouin, J. Gagnon, N. Boudreault and P.D. Harvey, Inorg. Chem., 33 (1994) 3689.
[162] P.D. Harvey, S.M. Hubig and T. Ziegler, Inorg. Chem., 32 (1994) 3700.
[163] J. Forniés, E. Lalinde, A. Martín and M.T. Moreno, J. Chem. Soc. Dalton Trans., (1994) 135.
[164] K. Matsumoto, M. Ikuzawa, M. Kamikubo and S. Ooi, Inorg. Chim. Acta, 217 (1994) 129.
[165] I.I. Moiseev, T.A. Stromnova and M.N. Vargaftik, J. Mol. Catal., 86 (1994) 71.
[166] J.L. Huggitt and D.M.P. Mingos, J. Chem. Soc. Dalton Trans., (1994) 1013.
[167] E. Furet, A. Le Beuze, J.-F. Halet and J.-Y. Saillard, J. Am. Chem. Soc., 116 (1994) 274.
[168] R. Bota, J. Chem. Soc. Dalton Trans., (1994) 2061.
[169] M. Bardají, A. Blasco, J. Jiménez, P.G. Jones, A. Laguna, M. Laguna and F. Merchán, Inorg. Chim. Acta, 223 (1994) 55.
[170] J.K. Burdett, O. Eisenstein and W.B. Schweizer, Inorg. Chem., 33 (1994) 3261.
[171] M.J. Calhorda and L.F. Veiros, J. Organomet. Chem., 478 (1994) 37.
[172] E. Cerrada, M.C. Gimeno, J. Jiménez, A. Laguna, M. Laguna and P.G. Jones, Organometallics, 13 (1994) 1470.
[173] M.C. Gimeno, J. Jiménez, P.G. Jones, A. Laguna and M. Laguna, Organometallics, 13 (1994) 2508.
[174] S.-J. Shieh, X. Hong, S.-M. Peng and C.-M. Che, J. Chem. Soc. Dalton Trans., (1994) 3067.
[175] R.M. Dávila, R.J. Staples and J.P. Fackler, Jr., Organometallics, 13 (1994) 418.
[176] A. Laguna, M. Laguna, J. Jiménez, F.J. Lahoz and E. Olmos, Organometallics, 13 (1994) 253
[177] U. Schubert, B. Mayer and C. Russ, Chem. Ber., 127 (1994) 2189.
[178] A. Antiñolo, F. Carrillo, B. Chaudret, M. Fajardo, J. Fernández-Baeza, M. Lanfranchi, H.-H. Limbach, M. Maurer, A. Otero and M.A. Pellinghelli, Inorg. Chem., 33 (1994) 5163.
[179] L. Weber, I. Schumann, H.-G. Stammler and B. Neumann, Chem. Ber., 127 (1994) 1349.
[180] I.L. Eremenko, H. Berke, B.I. Kolobkov and V.M. Novotortsev, Organometallics, 13 (1994) 244.
[181] G. Sánchez, F. Momblona, G. García, G. López, E. Pinilla and A. Monge, J. Chem. Soc. Dalton Trans., (1994) 2271.
[182] R.J. Salem and J.A. Ibers, Inorg. Chem., 33 (1994) 4216.
[183] I. Moldes, J. Ros, M.R. Torres, A. Perales and R. Mathieu, J. Organomet. Chem., 464 (1994) 219.
[184] W.-H. Sun, S.-Y. Yang, H.-Q. Wang, Q.-F. Zhou and K.-B. Yu, J. Organomet. Chem., 465 (1994) 263.
[185] W.-H. Sun, H.-Q. Wang, S.-Y. Yang, Q.-F. Zhou and K.-B. Yu, Polyhedron, 13 (1994) 389.
[186] J.-J. Peng, K.-M. Horng, P.-S. Cheng, Y. Chi, S.-M. Peng and G.-H. Lee, Organometallics, 13 (1994) 2365.
[187] S.-J. Chiang, Y. Chi, P.-C. Su, S.-M. Peng and G.-H. Lee, J. Am. Chem. Soc., 116 (1994) 11181.

[188] P. Braunstein, M. Knorr, M. Strampfer, Y. Dusausoy, D. Bayeul, A. DeCian, J. Fischer and P. Zanello, J. Chem. Soc. Dalton Trans., (1994) 1533.
[189] M.E. Barr, A. Bjarnason and L.F. Dahl, Organometallics, 13 (1994) 1981.
[190] H.-J. Haupt, U. Flörke and H.-G. Beckers, Inorg. Chem., 33 (1994) 3481.
[191] K. Onitsuka, X.-Q. Tao, W.-Q. Wang, Y. Otsuka, K. Sonogashira, T. Adachi and T. Yoshida, J. Organomet. Chem., 473 (1994) 195.
[192] M. Akita, M. Terada, N. Ishii, H. Hirakawa and Y. Moro-oka, J. Organomet. Chem., 473 (1994) 175.
[193] P. Mathur, M.M. Hossain and M.F. Mahon, J. Organomet. Chem., 471 (1994) 185.
[194] H.-C. Böttcher, B. Hartung, A. Krug and B. Walther, Polyhedron, 13 (1994) 2893.
[195] P. Braunstein, M. Knorr, M. Strampfer, A. Tripicchio and F. Ugozzoli, Organometallics, 13 (1994) 3038.
[196] C.E. Shuchart, A. Wojcicki, M. Calligaris, P. Faleschini and G. Nardin, Organometallics, 13 (1994) 1999.
[197] F. Bachechi, J. Organomet. Chem., 474 (1994) 191.
[198] F.H. Försterling and C.E. Branes, Organometallics, 13 (1994) 3770.
[199] P. Braunstein, D.G. Kelly, Y. Dusausoy, B. Bayeul, M. Lanfranchi and A. Tiripicchio, Inorg. Chem., 33 (1994) 233.
[200] D.V. Toronto, A.L. Balch and D.S. Tinti, Inorg. Chem., 33 (1994) 2507.
[201] B.H. Aw, K.K. Looh, H.S.O. Chan, K.L. Tan and T.S.A. Hor, J. Chem. Soc. Dalton Trans., (1994) 3177.
[202] I. Ara, J. Forniés, E. Lalinde, M.T. Moreno and M. Tomás, J. Chem. Soc. Dalton Trans., (1994) 2735.
[203] J.-C. Wang, Y. Chi, S.-M. Peng, G.-H. Lee, S.-G. Shyu and F.-H. Tu, J. Organomet. Chem., 481 (1994) 143.
[204] Y. Chi, C.-J. Su, L.J. Farrugia, S.-M. Peng and G.-H. Lee, Organometallics, 13 (1994) 4167.
[205] J.-H. Gong, D.-K. Hwang, C.-W. Tsay, Y. Chi, S.-M. Peng and G.-H. Lee, Organometallics, 13 (1994) 1720.
[206] J.T. Park, B.W. Woo, J.-H. Chung, S.C. Shim, J.-H. Lee, S.-S. Lim and I.-H. Suh, Organometallics, 13 (1994) 3384.
[207] I.L. Eremenko, H. Berke, A.A.H. van der Zeijden, B.I. Kolobkov and V.M. Novotortsev, J. Organomet. Chem., 471 (1994) 123.
[208] P. Mathur, M.M. Hossain and A.L. Rheingold, Organometallics, 13 (1994) 3909.
[209] J.T. Park, Y. Chi, J.R. Shapley, M.R. Churchill and J.W. Ziller, Organometallics, 13 (1994) 813.
[210] O.J. Curnow, J.W. Kampf, M.D. Curtis, J.-K. Shen and F. Basolo, J. Am. Chem. Soc., 116 (1994) 224.
[211] M.D. Curtis and O.J. Curnow, Organometallics, 13 (1994) 2489.
[212] U. Riaz, O.J. Curnow and M.D. Curtis, J. Am. Chem. Soc., 116 (1994) 4357.
[213] M.-T. Kuo, D.-K. Hwang, C.-S. Liu, Y. Chi, S.-M. Peng and G.-H. Lee, Organometallics, 13 (1994) 2142.
[214] B.R. Cockerton and A.J. Deeming, Polyhedron, 13 (1994) 1945.
[215] E.J. Voss, C.L. Stern and D.F. Shriver, Inorg. Chem., 33 (1994) 1087.
[216] T. Beringhelli, G. D'Alfonso and A.P. Minoja, Organometallics, 13 (1994) 663.
[217] J. Xiao, R.J. Puddephatt, L. Manojlović-Muir, K.W. Muir and A.A. Torabi, J. Am. Chem. Soc., 116 (1994) 1129.
[218] H.J. Kakkonen, M. Ahlgrén, T.A. Pakkanen and J. Pursiainen, J. Organomet. Chem., 482 (1994) 279.
[219] S.N. Dutta, R.-K. Kondru and P. Mathur, J. Organomet. Chem., 470 (1994) 169.
[220] J.R. Galsworthy, C.E. Housecroft, D.M. Matthews, R. Ostrander and A.L. Rheingold, J. Chem. Soc. Dalton Trans., (1994) 69.
[221] M.M. Harding, B. Kariuki, A.J. Mathews, A.K. Smith and P. Braunstein, J. Chem. Soc. Dalton Trans., (1994) 33.
[222] W.-H. Sun, H.-Q. Wang, Q.-F. Zhou, S.-Y. Yang and K.-B. Yu, Organometallics, 13 (1994) 2910.
[223] P. Braunstein, J. Rosé, D. Toussaint, S. Jääskelainen, M. Ahlgren, T.A. Pakkanen, J. Pursiainen, L. Toupet and D. Grandjean, Organometallics, 13 (1994) 2472.
[224] O. Rossell, M. Seco, R. Reina, M. Font-Bardia and X. Solans, Organometallics, 13 (1994) 2127.
[225] S.P. Tunik, V.R. Krym, G.L. Starova, A.B. Nikol'skii, I.S. Podkorytov, S. Ooi, M. Yamasaki and M. Shiro, J. Organomet. Chem., 481 (1994) 88.

[226] G. Bondietti, R. Ros, R. Roulet, F. Grepioni and D. Braga, J. Organomet. Chem., 464 (1994) C45.
[227] N. Nawar and A.K. Smith, Inorg. Chim. Acta, 227 (1994) 79.
[228] T. Adatia, H. Curtis, B.F.G. Johnson, J. Lewis, M. McPartlin and J. Morris, J. Chem. Soc. Dalton Trans., (1994) 1109.
[229] C. Cathey, J. Lewis, P.R. Raithby and M.R. de Arellano, J. Chem. Soc. Dalton Trans., (1994) 3331.
[230] D. Seyferth, D.P. Ruschke, W.M. Davis, M. Cowie and A.D. Hunter, Organometallics, 13 (1994) 3834.
[231] R. Reina, O. Rossell, M. Seco, D. de Montauzon and R. Zquiak, Organometallics, 13 (1994) 4300.
[232] O. Rossell, M. Seco, G. Segalés, S. Alvarez, M.A. Pellinghelli and A. Tiripicchio, Organometallics, 13 (1994) 2205.
[233] R. Carreto, V. Riera, M.A. Ruiz, A. Tiripicchio and M. Tiripicchio-Camellini, Organometallics, 13 (1994) 993.
[234] J.R. Galsworthy, C.E. Housecroft and A.L. Rheingold, J. Chem. Soc. Dalton Trans., (1994) 2359.
[235] B.F.G. Johnson, J. Lewis, H. Curtis, T. Adatia, M. McPartlin and J. Morris, J. Chem. Soc. Dalton Trans., (1994) 243.
[236] R.D. Adams, T.S. Barnard, Z. Li, W. Wu and T. Yamamoto, Organometallics, 13 (1994) 2357.
[237] Z. Xu, S. Kawi, A.L. Rheingold and B.C. Gates, Inorg. Chem., 33 (1994) 4415.
[238] Y. Yamamoto and H. Yamazaki, Inorg. Chim. Acta, 217 (1994) 121.
[239] M. Shieh and Y.-C. Tsai, Inorg. Chem., 33 (1994) 2303.
[240] M.T. Bautista, P.S. White and C.K. Schauer, J. Am. Chem. Soc., 116 (1994) 2143.
[241] T. Blum, B.T. Heaton, J.A. Iggo, J. Sabounchei and A.K. Smith, J. Chem. Soc. Dalton Trans., (1994) 333.
[242] T. Adatia, H. Curtis, B.F.G. Johnson, J. Lewis, M. McPartlin and J. Morris, J. Chem. Soc., Dalton Trans., (1994) 3069.
[243] S. Chan and W.-T. Wong, J. Chem. Soc. Dalton Trans., (1994) 1605.
[244] Z. Akhter, S.L. Ingham, J. Lewis and P.R. Raithby, J. Organomet. Chem., 474 (1994) 165.
[245] L. Ma, S.R. Wilson and J.R. Shapley, J. Am. Chem. Soc., 116 (1994) 787.
[246] M.A. Aubart, J.F.D. Koch and L.H. Pignolet, Inorg. Chem., 33 (1994) 3852.
[247] R.A.T. Gould and L.H. Pignolet, Inorg. Chem., 33 (1994) 40.
[248] V.G. Albano, F. Azzaroni, M.C. Iapalucci, G. Longoni, M. Monari, S. Mulley, D.M. Proserpio and A. Sironi, Inorg. Chem., 33 (1994) 5320.
[249] B. Zhuang, B. Pan, L. Huang and P. Yu, Inorg. Chim. Acta, 227 (1994) 119.
[250] E. Brivio, A. Ceriotti, R.D. Pergola, L. Garlaschelli, F. Demartin, M. Manassero, M. Sansoni, P. Zanello, F. Laschi and B.T. Heaton, J. Chem. Soc. Dalton Trans., (1994) 3237.
[251] V.G. Albano, A. Fumagalli, F. Grepioni, S. Martinengo and M. Monari, J. Chem. Soc. Dalton Trans., (1994) 1777.